

3 Results

3.1 Structural Investigation of SNARE Proteins by Electron Paramagnetic Resonance Spectroscopy

Assembly of SNARE complexes is thought to be a key event on the path to membrane fusion. Temporal and structural information on the intermediates of this reaction is scarce. The crystallized SNARE complex is extremely stable and likely to resemble a final conformational state assumed concomitant with membrane fusion. Different from hemagglutinin, the viral fusion protein of influenza, which is trapped in a dead-end conformation (for a recent review see (Skehel & Wiley, 2000)), the SNARE complex can be disassembled again allowing the proteins to go through several cycles of assembly and disassembly. A detailed understanding of the structures of SNARE proteins and their complexes is likely to offer new insights into the pathway by which these proteins lead to membrane fusion.

In this first part of the study monomeric as well as homo- and heterooligomeric complexes of neuronal SNARE proteins were investigated using site-directed spin labeling in combination with circular dichroism and absorption spectroscopy. These investigations focused on two main questions 1.) Is the binary complex between syntaxin and SNAP-25 a possible precursor in SNARE complex assembly? and 2) Is there any structural evidence for loosely assembled complexes as would be predicted for a step-by-step assembly reaction? As outlined in the “Introduction” electron paramagnetic resonance spectroscopy is ideally suited to study local protein conformation (for review see (Hubbell *et al.*, 2000), (Hubbell *et al.*, 1996), (Hubbell *et al.*, 1998), and (Feix, 1998)).

The EPR measurements were performed in close collaboration with Ralf Langen at the University of Southern California, Los Angeles.

3.1.1 Individual SNAREs and SNARE Core Complexes in Solution

As a starting point for the EPR experiments we used recombinant versions of the cytoplasmic domain of synaptobrevin 2 (residues 1-96), the SNARE motif of syntaxin 1a (residues 183-262), and the full-length version of SNAP-25 in which the four cysteines of the linker region were replaced with serines. Substitutions of single amino acid residues with cysteines were then performed by site-directed mutagenesis. Using the crystal structure of the core complex as a guide, residues were chosen that cover the full-length of the helix bundle and that represent buried, tertiary contact, and helix surface sites. Complexes were formed by appropriate monomer combination (Fasshauer *et al.*, 1997a). All proteins and complexes were purified to more than 95% purity by a combination of affinity and ion exchange chromatography (Fasshauer *et al.*, 1999) and labeled with the cysteine specific spin label (1-oxy-2,2,5,5-tetramethylpyrrolinyl-3-methyl)methanethio-sulfonate.

In the first set of experiments, a total of 12 sites were labeled in the two SNARE motifs of SNAP-25. Spectra were recorded from each of the SNAP-25 variants either as monomers or in core complexes with unlabeled synaptobrevin 2 and syntaxin 1a. Overlays of each of the corresponding spectra are shown in Fig. 5. From a detailed analysis of the spectra the following conclusions can be drawn. First, the spectra of all monomers were very similar to each other. Each spectrum was dominated by sharp and narrowly spaced peaks (central line width typically 2.5 G or less) that reflect a high degree of motion. Such high mobility is characteristic for unstructured regions ((Hubbell *et al.*, 2000), (Hubbell *et al.*, 1996), (Hubbell *et al.*, 1998), and (McHaourab *et al.*, 1996)). Second, profound spectral differences were observed in the core complex at each site, indicating the formation of an ordered structure. In general, the characteristic features of the individual spectra from the core complex are in excellent agreement with the crystal structure (Sutton *et al.*, 1998). For example, the lowest mobility is seen at positions 33, 47, and 49, i.e. sites that are buried in the crystal structure. Characteristic for immobile side chains are the strongly broadened lines and the increased separation between the outer peaks (see arrows in Fig. 5). In contrast, residues 20, 48, 79, 155, and 200 yielded spectra indicative of mobile side chains, although not as sharp as in the monomers (compare green and black traces in Fig. 5). Such spectra are typically seen at helix surface sites (McHaourab *et al.*, 1996), again in good agreement with their location in the crystal structure. All other sites exhibited intermediate

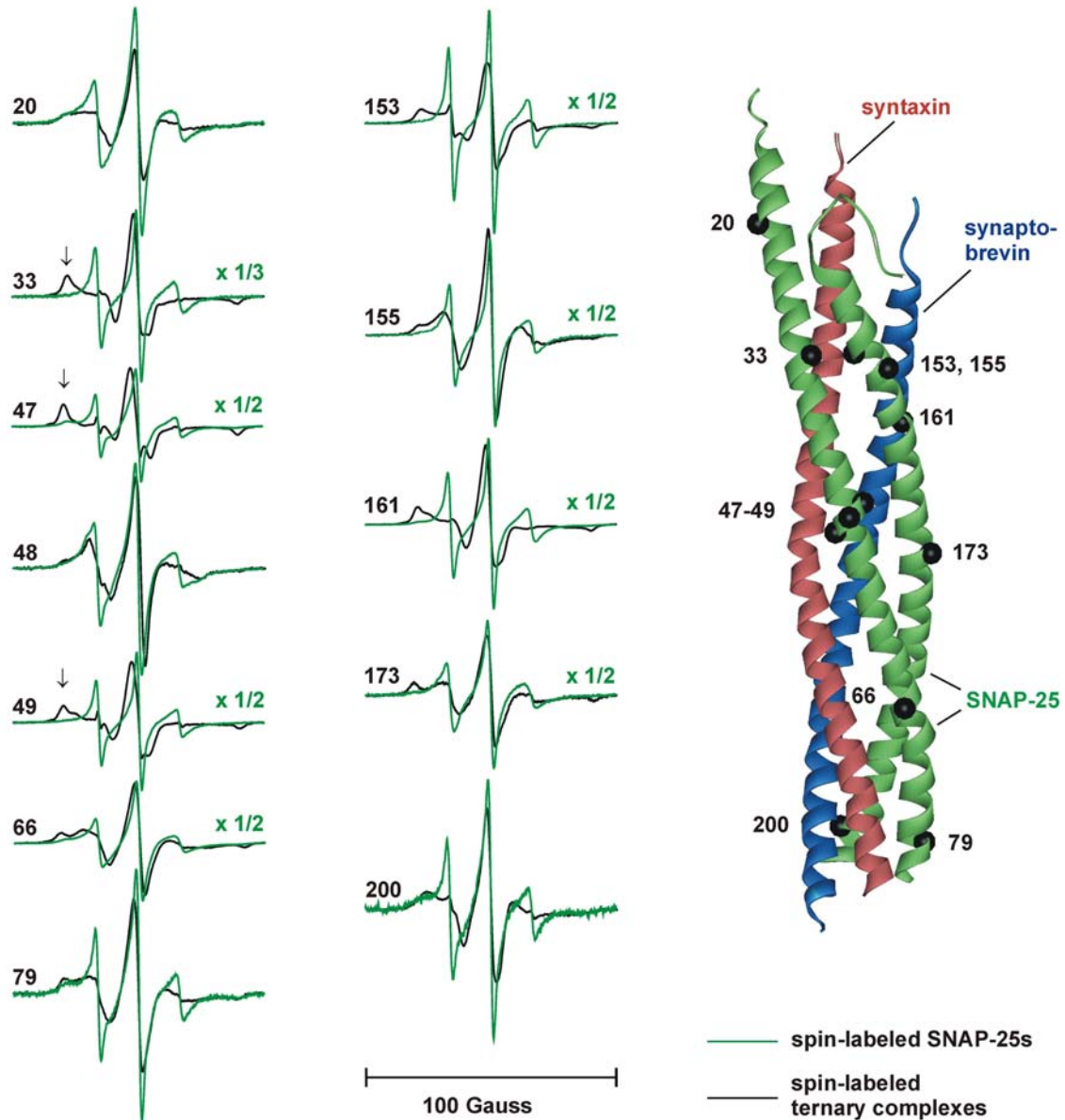


Fig. 5. EPR-spectra of spin labeled SNAP-25 variants in isolation or as part of ternary SNARE complexes. The positions in which spin labels were introduced are mapped on the crystal structure of the ternary complex (right). For each labeling position, spectra were recorded either in isolation (green) or after formation and purification of ternary complexes with synaptobrevin and the SNARE-motif of syntaxin (black). To facilitate comparison of the spectra, the amplitudes of the indicated spectra were multiplied with either 1/2 or 1/3.

Arrows indicate outer peaks characteristic for immobile side chains. Unless indicated otherwise, the scan width of these and all subsequent EPR spectra is 100 Gauss.

mobility and can be classified as tertiary contact sites (except for residue 173, which is unusually immobile for a helix surface site).

Furthermore, we determined the inverse second moment and the inverse central line width, for each of the SNAP-25 core complex spectra (Fig. 6). It was first shown for spin-labeled

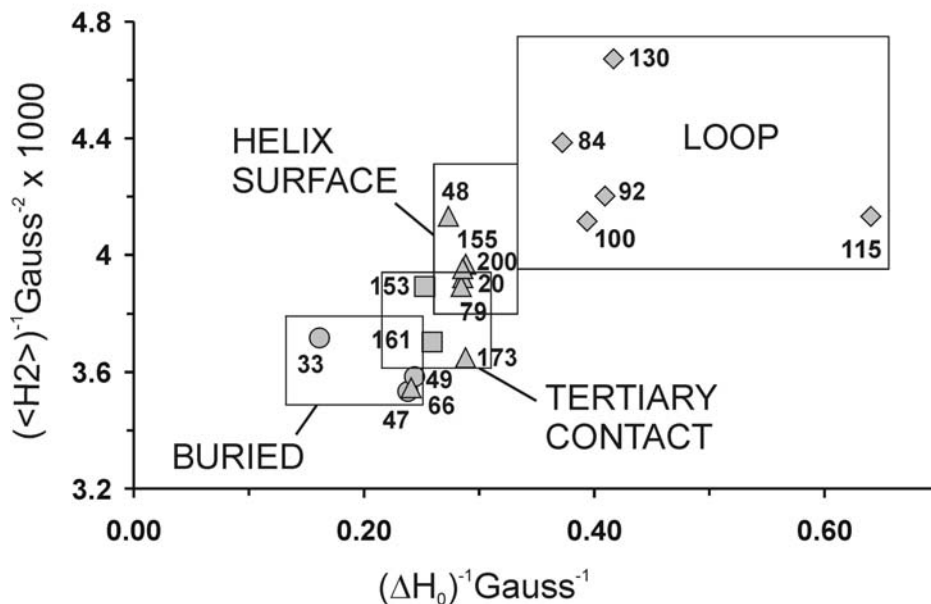
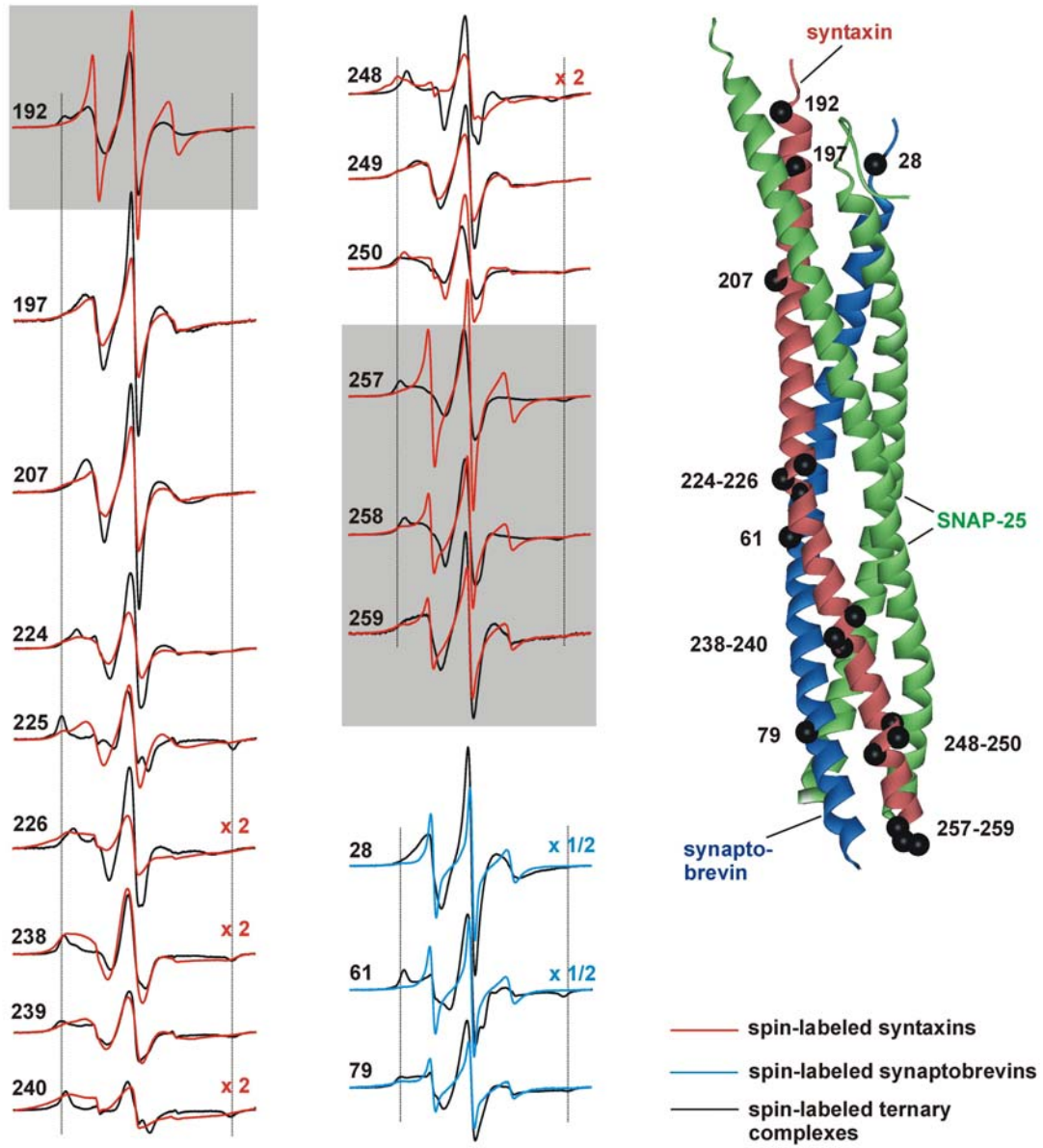
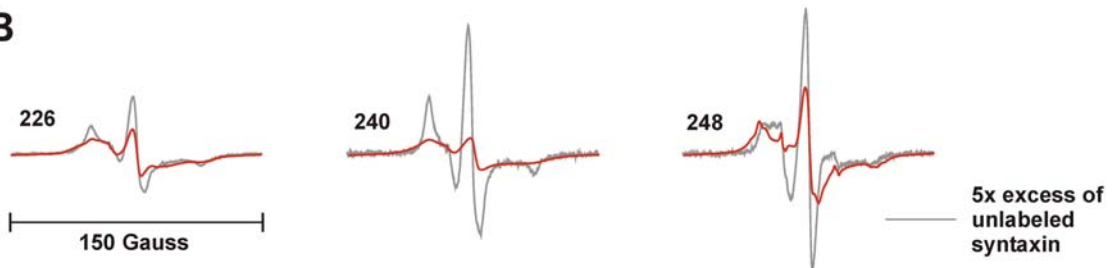


Fig. 6. Plot of reciprocal second moment ($\langle H^2 \rangle$) versus reciprocal central line width (ΔH_0) calculated from the EPR spectra of ternary complexes containing labeled SNAP-25 variants as shown in Fig. 5. Positions that in the crystal structure are in loop regions are indicated by diamonds, positions on helix surfaces by triangles, positions in tertiary contact by squares, and those being buried, i.e. pointing towards the interior of the helix bundle, by circles.

T4 lysozyme that the combined use of these mobility parameters provides an effective means for distinguishing between loop, surface, tertiary contact, and buried sites (McHaourab *et al.*, 1996). Reminiscent of the T4 lysozyme data, the respective sites in the core complex also cluster into different regions of the mobility plot in Fig. 6. These results further underscore the good agreement between the crystal structure and the site-directed spin labeling data.

Next, 15 different positions in the SNARE motif of syntaxin were individually labeled (Fig. 7). Unlike synaptobrevin and SNAP-25, the free SNARE motif of syntaxin was previously reported to be at least partially α -helical (Fasshauer *et al.*, 1998a). Furthermore, it is known to oligomerize ((Poirier *et al.*, 1998a), and (Fasshauer *et al.*, 1998a)). Spectral analysis of the spin-labeled free proteins revealed that only the outermost N- and C-terminal positions (residues 192 at one end and residues 257, 258, and 259 at the other) are mobile, whereas all other positions suggest the formation of a folded structure (Fig. 7). Generally, positions localized to the helix surface in the core complex also exhibited spectral characteristics of surface sites (residues 197, 207, 224, 225, 238, 239, 249, 250), suggesting that these residues again might be localized to the surface of a helix. For independent confirmation of syntaxin's secondary structure, we performed circular

A**B**

← **Fig. 7.** EPR spectra of spin labeled syntaxin (SNARE-motifs) and synaptobrevin variants in isolation or in ternary complexes

(A) Comparison of sets of spectra obtained from spin-labeled syntaxin and synaptobrevin variants. Spectra were recorded either in isolation (red, syntaxin; blue, synaptobrevin) or after formation and purification of ternary complexes (black). To facilitate comparison, the amplitudes of some of the spectra were multiplied with the factors indicated.

Vertical lines mark hyperfine extrema characteristic for immobilized spin label. Highly mobile spectra of syntaxin variants in isolation (red) are indicated by shaded areas.

(B) Spin-spin coupling in isolated SNARE motifs of syntaxin. Syntaxin variants spin labeled at positions 226, 240, and 248 were diluted with unlabeled syntaxin (~5-fold molar excess). Spectra of undiluted syntaxins are depicted in red, spectra of diluted syntaxins in black (dotted). The scan width is 150 Gauss. In all cases, addition of unlabeled syntaxin reduced spectral width and increased the amplitudes.

dichroism spectroscopy, which can be used at protein concentrations lower than required for EPR measurements. As shown in Fig. 8, the SNARE motif of syntaxin yielded a typical α -helical spectrum at 81 μ M but became increasingly unstructured upon dilution. Together, these data show that the SNARE motif of syntaxin is unstructured and monomeric (as confirmed by multiangle light scattering, not shown) at concentrations below 2 μ M and oligomerizes into helical bundles at increasing concentrations.

Interestingly, the spectra of all positions pointing inwards in the crystal structure of the core complex (residues 226, 240, 248) exhibited broadening beyond 100 G. Such broadening is a sign of strong spin-spin interactions that is observed only if the labeled positions are less than 15 Å apart (Hubbell *et al.*, 2000). Indeed, when unlabeled syntaxin was added, sharper peaks and narrowing of the spectra was observed (Fig. 7B). Thus, corresponding residues of the individual helices in the oligomer must be in close proximity at each of these labeling positions, which can only be reconciled with a parallel alignment of the helices. In addition, the side chains pointing inward in the core structure also point inward in the syntaxin homooligomer, indicating that the overall alignment of the helices is similar. At all other sites significantly weaker or no coupling was observed.

Next, EPR spectra were recorded from core complexes containing the spin labeled syntaxin derivatives (Fig. 7A, black spectra). Spectra from the N-terminal helix surface sites 192, 197, and 207 showed the characteristic features of helix surface sites. Also in good agreement with the crystal structure is the fact that inwardly pointing positions (226, 240, 248, and 257) exhibited highly immobile components.

The EPR spectra of C-terminal helix surface sites gave rise to uncharacteristically immobile components (residues 224, 225, 238, and 239) (Fig. 7). These are best explained by surface contacts between several SNARE complexes. Such oligomer formation was previously reported ((Poirier *et al.*, 1998a), and (Fasshauer *et al.*, 1998a)) (Table 3).

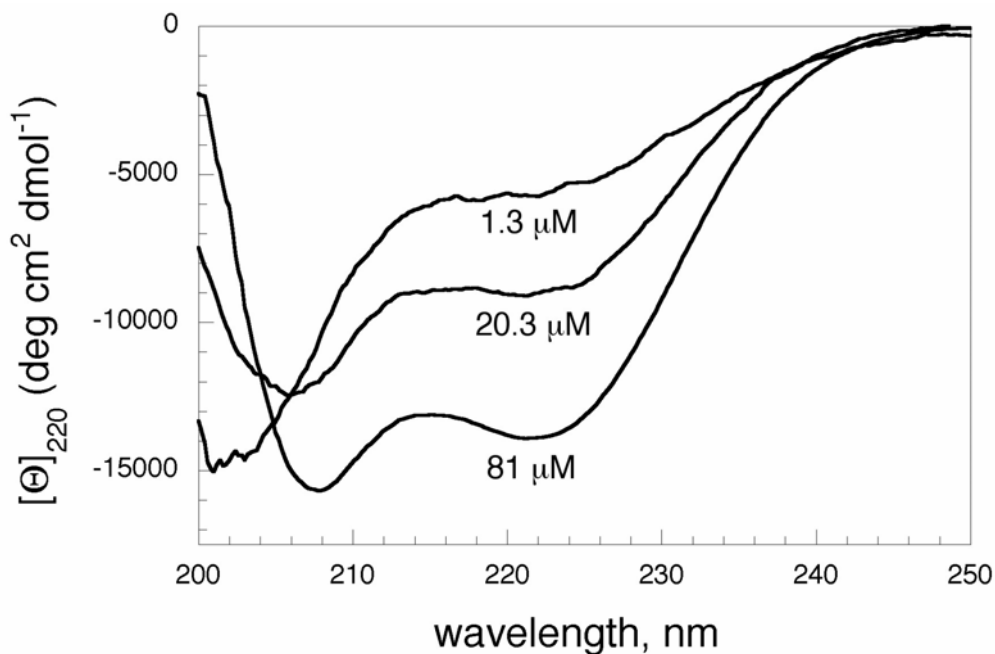


Fig. 8. Progressive decrease in α -helicity upon dilution of syntaxin SNARE motifs. CD-spectra were recorded at three different protein concentrations (40 mM sodium phosphate buffer). Note that in this experiment a slightly longer fragment of syntaxin was used (residues 180-262 instead of 183-262).

complex	theoretical mass [kDa]	measured mass [kDa]
binary complex	49.3	54.1 \pm 1.5
ternary complex without SNAP-25 loop	41.2	79.3 \pm 0.8
ternary complex	44.4	88.8 \pm 1.3
ternary complex TeNT	41.8	46.5 \pm 1.0
ternary complex BoNT/C	43.3	43.3 \pm 1.0

Table 3. Comparison of the molecular weights of various complexes determined by multiangle laser light scattering and the theoretical weights of monomers.

Moreover, in the crystal structure three asymmetrically arranged complexes were formed per unit cell that form contacts in the C-terminal region. To examine whether neighboring positions in the adjacent synaptobrevin helix are affected in a similar manner, we generated three spin-labeled derivatives of synaptobrevin. As shown in Fig. 7, only the spectrum of the most N-terminal labeling position (residue 28) was typical for a helix surface localization, whereas immobile peaks were observed both at positions 61 and 79, with position 61 being more pronounced. In synaptobrevin monomers, all three positions were highly mobile, in agreement with the notion that free synaptobrevin is unstructured. Interestingly, the spectrum of position 225 of syntaxin shows no mobile component,

although this residue has no side-chain contacts in the crystal structure of one of the three complexes in the unit cell. A tertiary contact with the loop connecting the two SNARE motifs of SNAP-25 (which were removed for crystallization, see below) can be excluded, because removal of the loop did not change the spectrum (not shown). These findings suggest that the oligomeric interactions in solution may be somewhat different from that in the crystal.

The data described so far demonstrate that the structural features of the ternary complex in solution as determined by EPR spectroscopy are in good agreement with the crystal structure. The only exception relates to an oligomeric interaction between complexes that involves the C-terminal regions of all four helices and that is not matched by corresponding crystal contacts. Furthermore, the data confirm that the monomeric forms of synaptobrevin and SNAP-25 are unstructured over the entire length of the SNARE motif, whereas the SNARE motif of syntaxin forms oligomeric helical bundles at higher concentrations in which each helix appears to have an orientation with respect to surface exposure and buried residues that is similar to the ternary complex. Together with a previous report (Poirier *et al.*, 1998b), these findings validate the spin labeling approach as a powerful tool for the study of SNARE structure and enabled us to determine features of the SNAREs for which structural information is not available.

3.1.2 Loop Region of SNAP-25

Previous data showed that the region of SNAP-25 connecting the two SNARE motifs is sensitive to proteases (Poirier *et al.*, 1998a), (Fasshauer *et al.*, 1998a), and it was therefore not included in the crystallization of the core complex (Sutton *et al.*, 1998). To analyze its structure, several positions were labeled. The corresponding EPR spectra exhibit sharp and narrowly spaced lines (Fig. 9) suggesting that those sites are unstructured. To compare the mobility at these sites with that of sites in the core complex (Fig. 9) we again determined the inverse second moment and the inverse of the central line width mobility parameters. As shown in Fig. 9, residues 84, 92, 100, 115, and 130 cluster in the region of highest mobility.

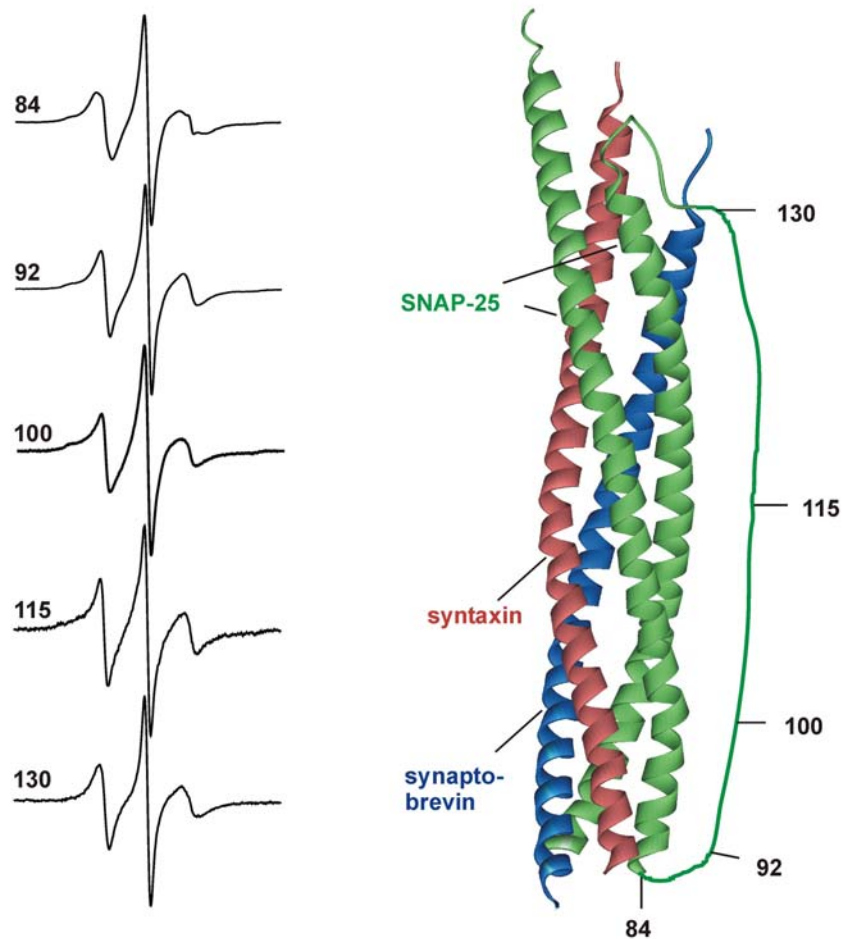


Fig. 9. Structure of the loop region of SNAP-25 in the ternary complex as determined by EPR-spectroscopy. The relative positions of the spin labeled residues are indicated on the right. Note that the loop connecting the two SNAP-25 helices is drawn schematically since it is not part of the crystal structure.

3.1.3 Core Complexes with Truncated SNAREs

We next investigated how C-terminal truncations of synaptobrevin and syntaxin affect the structure of the complex. Most importantly, we wanted to find out whether the perturbations of the complex structure caused by such a deletion remain local or whether they destabilize the complex in a more profound way. As outlined under “Discussion”, a distinction between these possibilities is relevant for an understanding of the SNARE assembly and disassembly mechanism. As a starting point, we deleted residues that are also cleaved off by certain clostridial neurotoxins. The following mutants were generated: a syntaxin variant shortened by nine residues (residues 183-253, the latter corresponding to the cleavage site of botulinum neurotoxin/C), and a synaptobrevin variant shortened by 20 amino acids (residues 1-76, corresponding to the fragment generated by tetanus

neurotoxin). With these mutants, sets of spin labeled complexes were formed that were analyzed by EPR spectroscopy (Fig. 10).

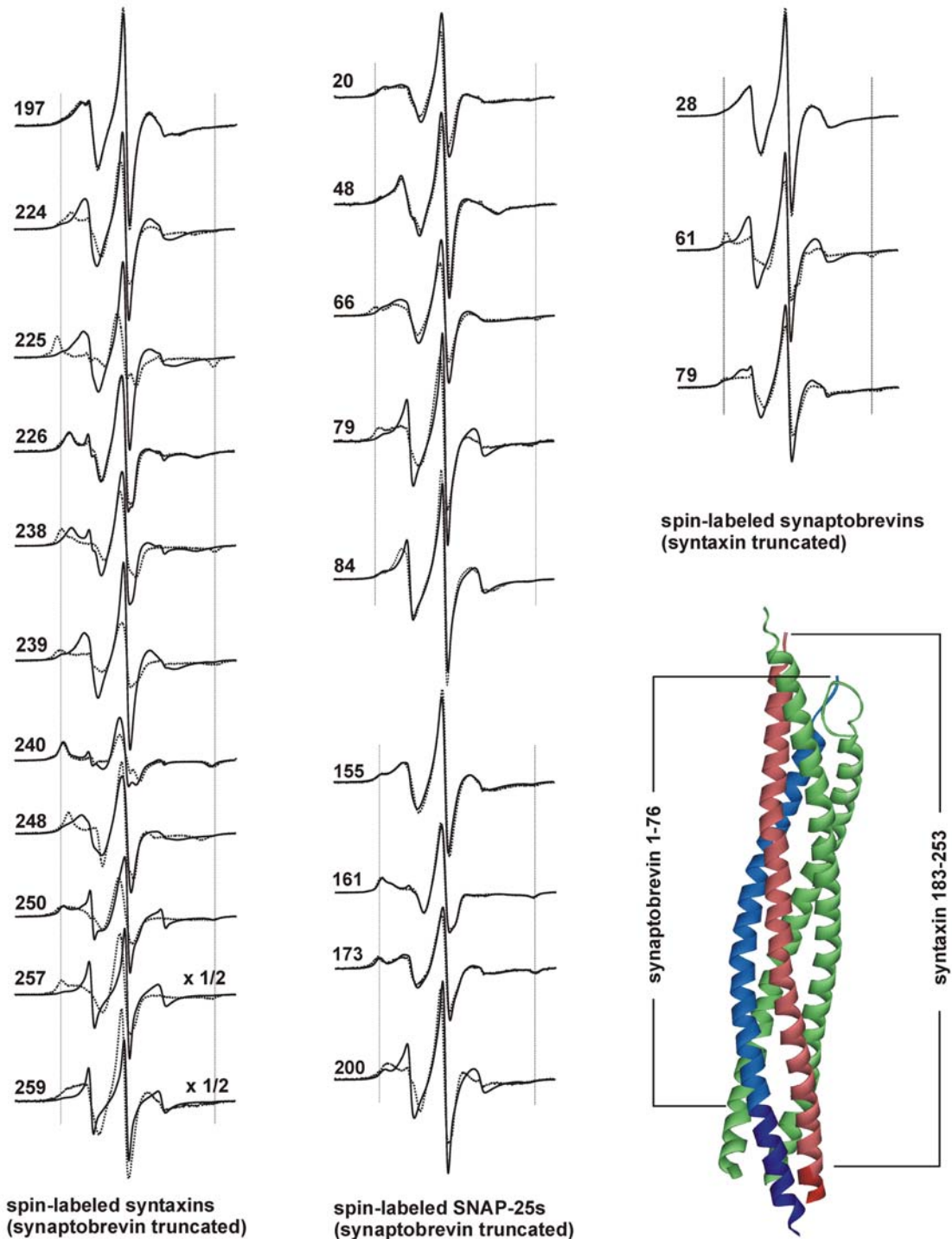


Fig. 10. EPR-spectra of ternary complexes containing truncated SNAREs.

Ternary complexes containing spin labeled SNAREs were formed that contained either truncated synaptobrevin (residues 1-76) or syntaxin (residues 183-253) (see scheme bottom right). For comparison, the corresponding spectra derived from the non-truncated complexes are indicated (dotted lines, data from Figs. 5 and 7). The amplitudes of spectra with sharp peaks (257 and 259) were multiplied by 1/2.

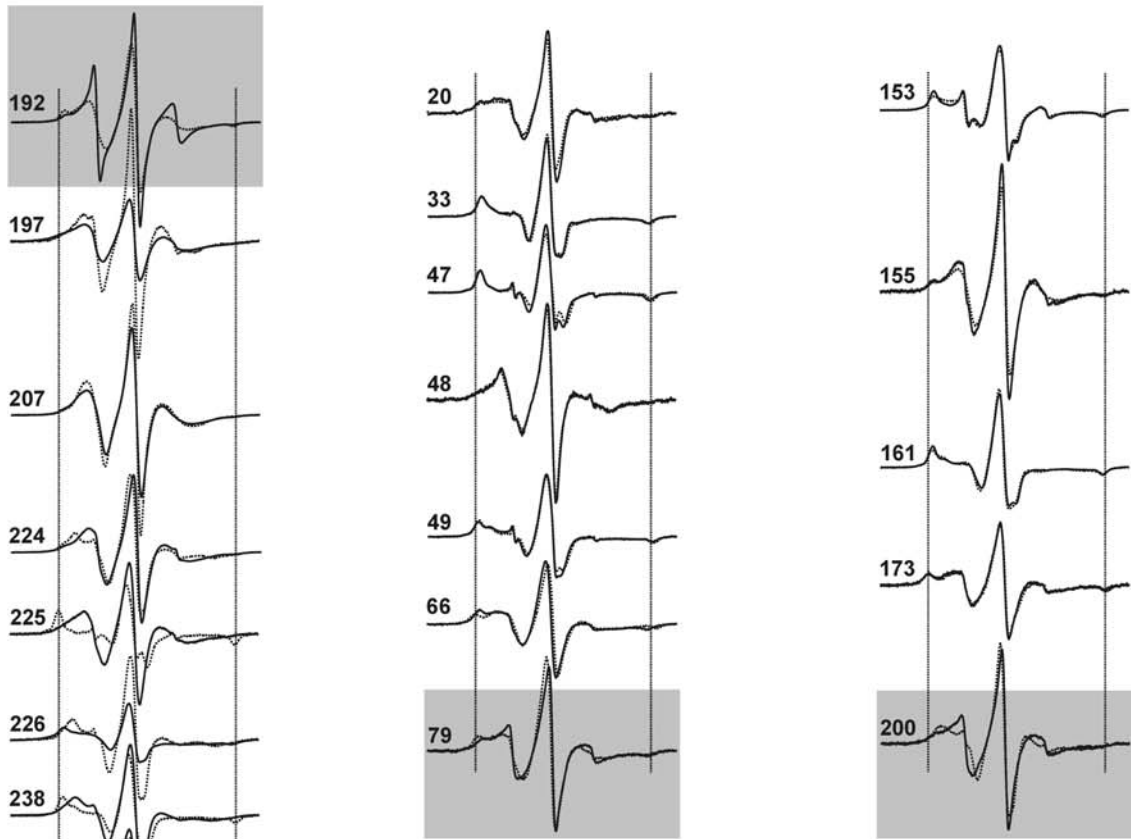
When the corresponding spectra of intact and truncated complexes were compared, several interesting features became apparent. Unlike in the intact complex, no evidence for contact sites was found at C-terminal surface positions, suggesting that truncated complexes do not oligomerize. Immobile components in surface positions of syntaxin (e.g. positions 224, 225, and 239), synaptobrevin (positions 61 and 79), and a single position in SNAP-25 (position 66) largely disappeared and gave rise to typical helix surface spectra, similar to those of the N-terminal surface positions that remained unaltered. The monomeric state was confirmed by size-exclusion chromatography and multiangle laser light scattering (Table 3).

Moreover, inwardly pointing residues (e.g. positions 226 and 240) located above the truncation site remained unaltered, documenting that the structure of the helical bundle is preserved N-terminal of the truncation site (Fig. 10). These data agree with other findings such as thermal stability and CD spectroscopy, which indicate that such truncations do not cause major overall changes in complex structure and stability. Finally, labeling positions located in stretches of syntaxin and SNAP-25 that are C-terminal of the cleavage site in synaptobrevin yielded mobile spectra (Fig. 10), including residues 257 and 259 of syntaxin, residues 79 and 84 of SNAP-25 (N-terminal helix), and residue 200 of SNAP-25 (C-terminal helix). We conclude that the ends of the three helical segments collapse into random helical coils when the fourth partner is missing.

3.1.4 Binary Complex between Syntaxin and SNAP-25

In the next set of experiments, we investigated the structure of the binary complex formed by syntaxin and SNAP-25. Previous work has shown that in the absence of synaptobrevin these two proteins form a complex with a 2 (syntaxin): 1 (SNAP-25) stoichiometry that is also α -helical but less stable than the ternary complex (Fasshauer *et al.*, 1997b). Addition of synaptobrevin to such binary complexes results in the formation of ternary complexes, effectively displacing one of the syntaxin molecules. Because SNAP-25 and syntaxin are both localized in the plasma membrane, it is possible that such binary complexes form in the membrane and represent the physiological acceptor site for synaptobrevin upon vesicle docking.

Again we generated sets of complexes containing labeled SNAP-25 and syntaxin variants. When the SNAP-25 spectra of the binary complexes were compared with those of the corresponding ternary complexes, most of the labeling positions were found to be nearly

A

spin-labeled SNAP-25s

B

spin-labeled syntaxins

← **Fig. 11.** EPR spectra of binary complexes containing syntaxin and SNAP-25

(A) Comparison of sets of spectra containing spin-labeled syntaxins or spin labeled SNAP-25 variants. In each case, the binary complexes containing labeled variants were purified. For comparison, the corresponding spectra derived from the ternary complexes are indicated (dotted lines, data from Figs. 5 and 7). Shaded areas indicate spectra that are highly mobile in the binary complex.

(B) Spin-spin coupling of syntaxin in the binary complex. Syntaxin variants spin labeled at positions 197, 226, and 248 were diluted with unlabeled syntaxin and combined with excess of SNAP-25 for complex formation. All spectra were recorded without further purification of the complexes. Spectra of complexes containing undiluted, labeled syntaxins are represented by dotted lines, spectra of complexes containing mixtures of labeled and unlabeled syntaxins are represented by solid lines. The scan width is 150 Gauss.

identical (Fig. 11). These findings show that the structures of the two SNAP-25 helices closely resemble those of the ternary complex. The only significant differences are observed at the C-terminal ends of both helices (residues 79 and 200). Here the spectra indicate a higher degree of mobility. In contrast, the differences between the syntaxin spectra of the binary and ternary complexes were more profound. It should be borne in mind that the syntaxin spectra have contributions from two syntaxins and it is therefore not straightforward to assign the EPR spectra to individual syntaxins. Most importantly, labeling positions pointing inward in the complex are not only immobile but also show varying degrees of spin-spin coupling (residues 226 and 248) (Fig. 11A). Thus, residues pointing inward in the ternary complex also point inward in the binary complex, and because the corresponding amino acids are always close to each other, the two syntaxin helices must be oriented in parallel. With the exception of position 197, no spin-spin coupling was observed in labeling positions that do not point to the interior of the bundle. These observations were confirmed when increasing amounts of unlabeled syntaxin and SNAP-25 were added during complex formation (Fig. 11B). Spin-spin coupling disappeared whereas the overall character of the spectra remained unchanged.

To confirm the parallel alignment of the two syntaxins with an independent approach, we labeled position 197 of syntaxin with the dye Alexa 594 (labeling efficiency >80%, data not shown). The absorption spectrum of binary complexes containing dye-labeled syntaxin showed a maximum at 590 nm and a second peak at 554 nm (Fig. 12). Addition of unlabeled synaptobrevin (Fig. 12) or of unlabeled syntaxin (not shown) resulted in a significant reduction of the maximum at 554 nm, yielding a spectrum very similar to that of free dye. We conclude that the increased absorption at 554 nm is due to an interaction between adjacent chromophores that disappears upon displacement of one (or both) of the labeled syntaxins. The parallel alignment of both syntaxin molecules in the neuronal binary complex is compatible with the orientation needed for assembly in the plane of a

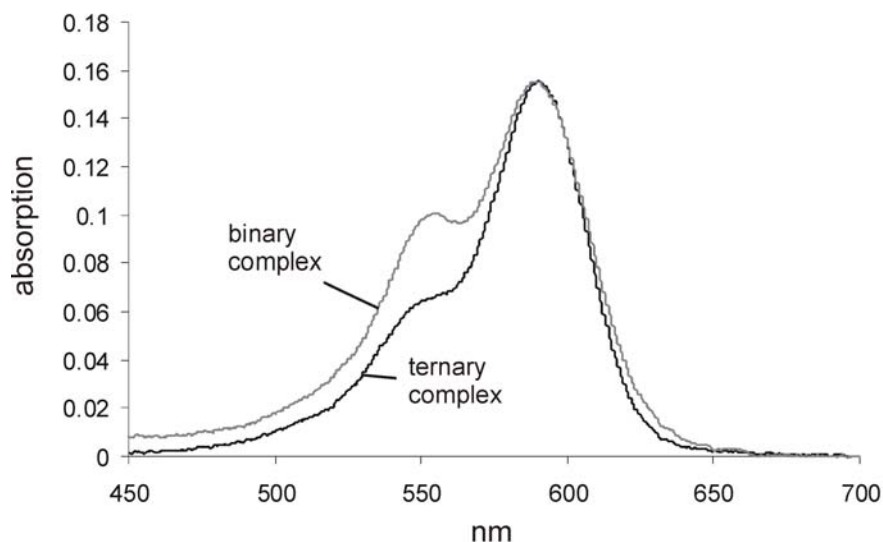


Fig. 12. Absorption spectra of binary- and ternary complexes (protein concentration 1.32 μ M, containing syntaxin that is labeled at position 197 with Alexa594-maleimide. Ternary complex was formed by addition of 10-fold molar excess of synaptobrevin.

membrane, in agreement with the notion that this complex may serve as an intermediate in SNARE assembly-disassembly pathways.

EPR spectra of surface positions in the C-terminal region were more similar (i.e. more mobile) to the truncated complex than to the intact ternary complex suggesting that the binary complex does not form oligomers. This conclusion was confirmed by size exclusion chromatography and multiangle laser light scattering (Table 3). Finally, a high degree of mobility was found at the N- and C-terminal positions (residues 192 and 257-259). The latter corresponds to the higher mobility of the adjacent residues of SNAP-25, suggesting that the C-terminal end (corresponding to the region around layer 8 of the core complex) of the binary complex is unstructured. We conclude that the structure of the binary complex is similar to that of the ternary complex, representing an elongated and almost completely folded bundle of four α -helices in which one syntaxin molecule substitutes for synaptobrevin.

3.2 Conformational Changes of the N-terminal Domain of Syntaxin and Their Influence on SNARE Complex Assembly

3.2.1 Preliminary Remarks

As outlined in the Introduction, two different conformations of syntaxin have been described, referred to as “open” and “closed” (Fig. 13). In the “open” conformation, the N-terminally located three-helix bundle is tethered to the H3-domain only by the connecting stretch of amino acids and appears to be mobile with respect to the remainder of the molecule. This conformation is assumed when syntaxin is in complex with its SNARE-partners (Hanson *et al.*, 1997b). In the “closed” conformation, parts of the helical H3-domain fold into the groove formed on the surface of the N-terminal tri-helix bundle, with the connecting stretch being folded, consisting of a sequence of ordered short α -helices and turns. This conformation is seen in the complex with munc-18 as highlighted in the recently solved crystal structure (Misura *et al.*, 2000). As expected, syntaxin bound to munc-18 cannot form SNARE complexes (Yang *et al.*, 2000) since a major part of the H3-domain is buried. Several previous studies also addressed the relation of the N-terminal with the H3 domain in free, i.e. uncomplexed syntaxin ((Calakos *et al.*, 1994), (Hanson *et al.*, 1995), and (Dulubova *et al.*, 1999)). Although no high-resolution structure is available, these studies allowed for the conclusion that free syntaxin also assumes the “closed” conformation. Detailed kinetic studies on the yeast syntaxin Sso1p showed that formation of binary complexes with the yeast SNAP-25 Sec9p was slow (Nicholson *et al.*, 1998). Removal of the N-terminal domain accelerated the binding rate approximately 2000-fold, in agreement with the view that the free Sso1p is in the “closed” conformation and thus incapable of efficient assembly with its SNARE partners. Once binary complexes are formed, the synaptobrevin homologue Snc1p bound rapidly indicating that formation of binary complexes is rate-limiting.

Together, these data show that the transition between open and closed conformation may represent an important regulatory step that controls the reactivity of syntaxin towards its SNARE partners and thus regulates membrane fusion. A refined understanding of the conformations of neuronal syntaxin is therefore of high importance for shedding light on a potential control mechanism of exocytosis. Here several complementary approaches, all based on the selective labeling of syntaxin variants or of its SNARE partners with fluorophores, were pursued in order to clarify the conformational dynamics of syntaxin.

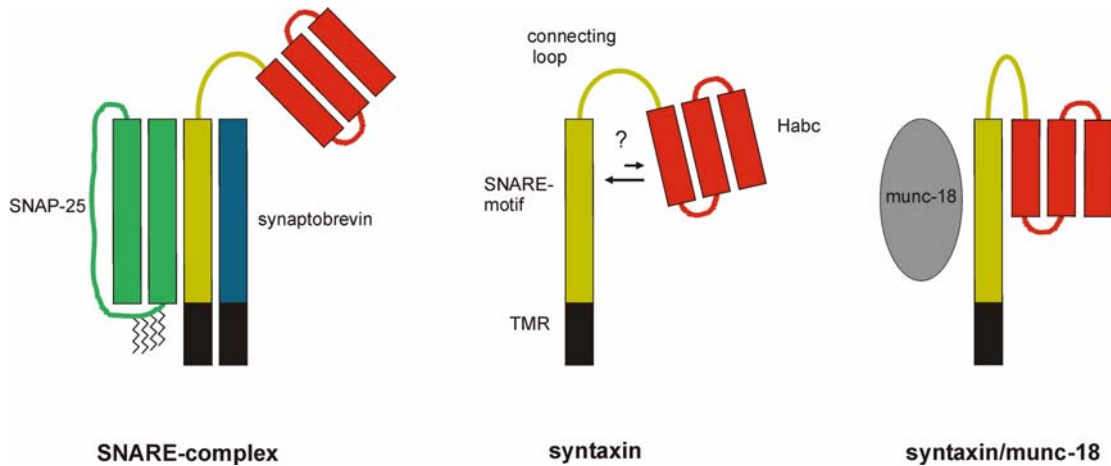


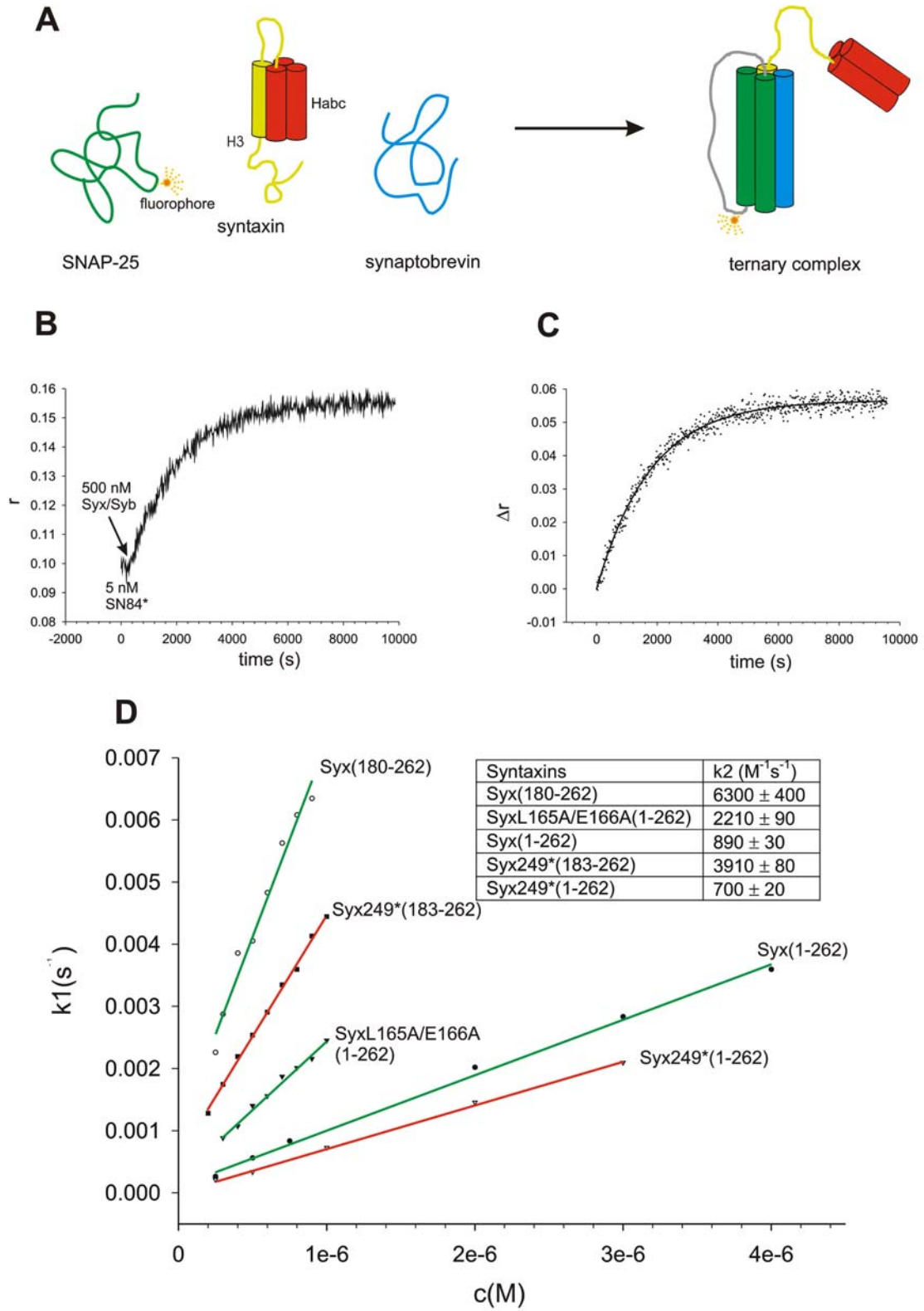
Fig. 13. Transition between open and closed conformations of syntaxin
 The Habc domain (red) of syntaxin has the potential to fold back onto its SNARE motif (yellow, boxed). Two different conformations of syntaxin are known: open (left) when in complex with synaptobrevin (blue) and SNAP-25 (green) and closed (right) when in complex with munc-18 (gray). For isolated syntaxin (middle) it is thought that the closed state is predominant. No information is available on the interconversion between open and closed states.

3.2.2 Kinetics of SNARE Complex Formation Using Syntaxin Variants Containing or Lacking the N-terminal Regulatory Domain

In order to find out whether the N-terminus of syntaxin effects assembly of the neuronal SNARE complex to the same degree as the N-terminus of Sso1p, effects assembly of the yeast SNARE complex we established a new assay in which complex formation is monitored by a change in fluorescence anisotropy.

The association of a protein with one or more binding partners results in an increase in its rotational correlation time. If the protein is labeled with a fluorophore a concomitant increase in fluorescence anisotropy may be observed.

In an initial experiment SNAP-25 was labeled at position 84 with the fluorophore Alexa 488. Binding of unlabeled syntaxin and synaptobrevin resulted in the formation of a SNARE complex in which the fluorophore is positioned at the very start of the loop region connecting the two SNAP-25 helices (Fig. 14A, B). This position is highly mobile as determined by EPR spectroscopy (Fig. 9) and therefore unlikely to interfere with complex formation. Addition of syntaxin and synaptobrevin caused a significant increase in anisotropy (0.10-0.16). A 100-fold excess of syntaxin and synaptobrevin over SNAP-25 was used to ensure that it is only the concentration of SNAP-25 that changes significantly during the reaction. The obtained curve fit well with a monoexponential rise function and



← **Fig. 14.** A kinetic study of ternary complex formation

(A) The cartoon illustrates the assembly of a ternary complex between SNAP-25 (green), synaptobrevin (blue), and syntaxin (Habc domain (red), H3 domain and connecting loop (yellow)). A fluorescent marker is attached to SNAP-25. Complex formation can be monitored by a change in fluorescence anisotropy.

(B) Raw data of a reaction in which SNAP-25 is labeled with Alexa488-maleimide at position 84. The addition of 500 nM Syx(1-262)/Syb(1-96) to 5 nM SNAP-25 results in an increase in anisotropy (r) that is monitored over time.

(C) The change in anisotropy (Δr) is plotted against time and the resulting curve fitted by a mono exponential rise function. A first order rate constant (k_1) is obtained.

(D) The first order rate constants determined for reactions with different concentrations (of excess unlabeled proteins) are plotted against the corresponding concentrations. The slope of each resulting line yields the second order rate constant for that reaction. Green lines represent linear fits for assembly reactions in which SNAP-25 was labeled and increasing concentrations of Syb/Syx(180-262), Syb/SyxL165A/E166A(1-262), or Syx/Syb(1-262) were added. Red lines represent linear fits for assembly reactions in which syntaxin was labeled (Syx249(183-262) or Syx249(1-262)) and increasing concentrations of synaptobrevin and SNAP-25 were added. Proteins that are labeled with Alexa488-maleimide are marked by an asterisk.

the pseudo first order rate constant was derived (Fig. 14C). A series of experiments was carried out in which the concentrations of synaptobrevin and syntaxin were increased. The pseudo first order rate constants were plotted against the corresponding concentrations and the second order rate constant determined from the slope (Fig. 14D). Interestingly, complex formation is much faster than in the yeast system. When binary complex formation between syntaxin and SNAP-25 was studied (not shown) a similar rate constant as for ternary complex formation was observed ($820 \pm 20 \text{ M}^{-1} \text{ s}^{-1}$ for binary opposed to $890 \pm 30 \text{ M}^{-1} \text{ s}^{-1}$ for ternary complex formation), indicating that binding of synaptobrevin must be rapid.

Next, we asked whether removal of the N-terminus of syntaxin speeds up the assembly reaction. Again, complex formation was followed at increasing concentrations of syntaxin and synaptobrevin. The change in anisotropy was equivalent to that seen for the full-length complex. The determined second order rate constant is about seven-fold higher than the one observed for full-length syntaxin, but in the same range as the one determined for the equivalent binary complex in yeast.

Previously, Rizo and coworkers described a double mutant of syntaxin (L165A/E166A), which is thought to exist in an open conformation (Dulubova *et al.*, 1999). We tested the kinetic behavior of complex formation applying this mutant in our assay. A second order rate constant was determined ($2210 \pm 90 \text{ M}^{-1} \text{ s}^{-1}$) that lies between the previous two values ($6300 \pm 400 \text{ M}^{-1} \text{ s}^{-1}$ for Syx(180-262) and $890 \pm 30 \text{ M}^{-1} \text{ s}^{-1}$ for Syx(1-262)). The N-terminus appears to cause steric constraints on the assembly reaction.

To test whether the same kinetics is observed when instead of SNAP-25 syntaxin is labeled, we covalently attached Alexa488-maleimide at position 249 of the full- (1-262)

and the short- (183-262) cytoplasmic versions of the protein. EPR measurements indicated that this position is on the helix surface and has no tertiary contacts (Fig. 7). Therefore, we expected little interference with complex formation. This time, unlabeled synaptobrevin and SNAP-25 were added in at least 40-fold molar excess. For both syntaxins (Syx(1-262) and Syx(183-262)) anisotropy changed from 0.10 to 0.20. Consequently, both constructs gave an excellent read out. The determined second order rate constants compare well with the ones determined with labeled SNAP-25. The deviations are within the experimental error and could arise from minor effects of the labels on assembly kinetics. This time the presence of the N-terminus slows down complex formation by a factor of 5. We conclude that the N-terminus of syntaxin causes a small, yet significant inhibition of complex formation.

Previously, the interaction between both syntaxin domains (residues 4-193 and residues 194-267) was studied by surface plasmon resonance spectroscopy (Calakos *et al.*, 1994). The K_d value determined was 4.1 μM . We now asked whether the isolated N-terminal domain of syntaxin has an effect on ternary complex formation. For this purpose, synaptobrevin and the N- and C-terminal domains of syntaxin were preincubated for three hours on ice and then added to A488- labeled SNAP-25. Again, complex formation was monitored by a change in fluorescence anisotropy (Fig. 15). Interestingly, the N-terminal domain of syntaxin 1a had no effect on ternary complex formation, since in its absence the kinetics was unaltered. When Syx249 (180-262) was labeled and the other SNARE components were added a similar result was obtained; the N-terminal domain did not interfere with complex formation (data not shown). Since the C-terminal fragment of syntaxin used in this study is bigger than the one used in the plasmon resonance study and thus offers more contact area to the Habc-domain a stronger interaction was expected. That this is not the case might be due to dextran-surface contacts in the plasmon resonance study. All our attempts to detect an interaction between the two isolated domains of syntaxin failed, including nondenaturing gel electrophoresis, multi angle laser light scattering and circular dichroism spectroscopy (data not shown). Therefore, we conclude that both domains need to be connected in order to interact.

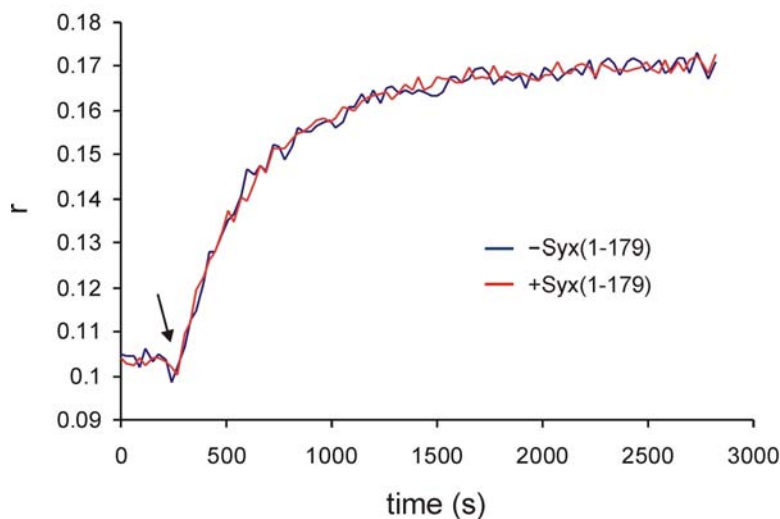


Fig. 15. The isolated N-terminus of syntaxin has no influence on SNARE complex assembly. Ternary complex formation between SNAP-25 (5 nM SNAP-25 labeled at position 84 with Alexa488-maleimide) and a mixture of synaptobrevin and syntaxin's H3 domain (500 nM Syb/Syx(180-262)) was monitored by an increase in fluorescence anisotropy (r) (see also Fig. 14B). When the N-terminus of syntaxin (5 μ M Syx(1-179)) was present during assembly (red trace) a similar trace was observed as when it was absence (blue trace).

3.2.3. Analysis of Syntaxin Conformations by Single Molecule Fluorescence Spectroscopy

3.2.3.1 General Remarks

The results described above cannot be easily reconciled with the view that free syntaxin assumes the “closed” conformation. First, removal of the N-terminal domain including the connecting region accelerated SNARE-complex formation only moderately, in stark contrast to the corresponding rates of the yeast relative Sso1p. It is conceivable that binding between the N-terminal domain and the SNARE-motif is not as tight as suggested by the structure of syntaxin in the munc-18 complex. Second, we did not find evidence for an interaction of the free N-terminal domain with the rest of the molecule when the experiments were carried out in solution, again suggesting that the interaction between these domains (if any) is weak.

To shed light on the conformational dynamics of free syntaxin, we developed a novel approach that is based on dual labeling of individual syntaxin molecules with two different fluorophores, followed by fluorescence spectroscopy of single molecules. These experiments were carried out in close collaboration with Enno Schweinberger, Jerker Widengren and Claus Seidel from the spectroscopy department at the Max-Planck-Institute

for biophysical Chemistry, Göttingen. The fluorophores were chosen for their suitability in fluorescence resonance energy transfer (FRET), in which energy from the excited state of the higher-energy (donor) fluorophore is transferred to the lower energy (acceptor) fluorophore, resulting both in a shortening of the lifetime of the donor and in an increased emission of the acceptor fluorophore. Since FRET is highly dependent on the distance of the fluorophores, it can be used to map distances between different labeling positions.

3.2.3.2 The Open Conformation of Syntaxin

In a first set of experiments four double mutants of syntaxin were generated in which the native amino acids were substituted by cysteines. The positions were chosen based on the crystal structure of syntaxin in complex with munc-18 (Misura *et al.*, 2000). In this structure all labeling positions are on the surface of the helix backbone and (when positioned in the H3 domain) have no direct contact with the Habc domain. Therefore, if a closed structure of isolated syntaxin resembles that of syntaxin in complex with munc-18 interference of the fluorescent label with back folding of the protein should be minimal. Position 91 was fixed while the second position varied and encompassed amino acids 225, 207, 197, and 59 (Fig. 16). Amino acids 91 and 59 reside in the Habc domain only. This double mutant was chosen to serve as a control, because the Habc domain is thought to be independently folded and extremely stable. Thermal melts using circular dichroism indicated that the three-helix bundle unfolds at temperatures above 80°C (unpublished observations, Dirk Fasshauer). If structural flexibility in the protein backbone between two labeled cysteines is compromised it is most likely in this domain.

Labeling of the proteins with the fluorescent dyes Alexa488- and Alexa594-maleimide resulted in a heterogeneous mixture in which some proteins were labeled with the donor some with the acceptor and others with both donor and acceptor. Considering that some mutants may be labeled at only one position a theoretical set of eight different fluorescent species is possible. Only two of them, namely the donor/acceptor, and acceptor/donor pairs are FRET active. In general, we assumed that these are equivalent pairs and that the local protein environment does not have a significant influence on whether the two dyes are exchanged in their positions. To differentiate the two species is not easy on the single molecule level. If it were it would automatically hint toward a preferential interaction of the dyes with the protein backbone. The fluorescence anisotropy information obtained

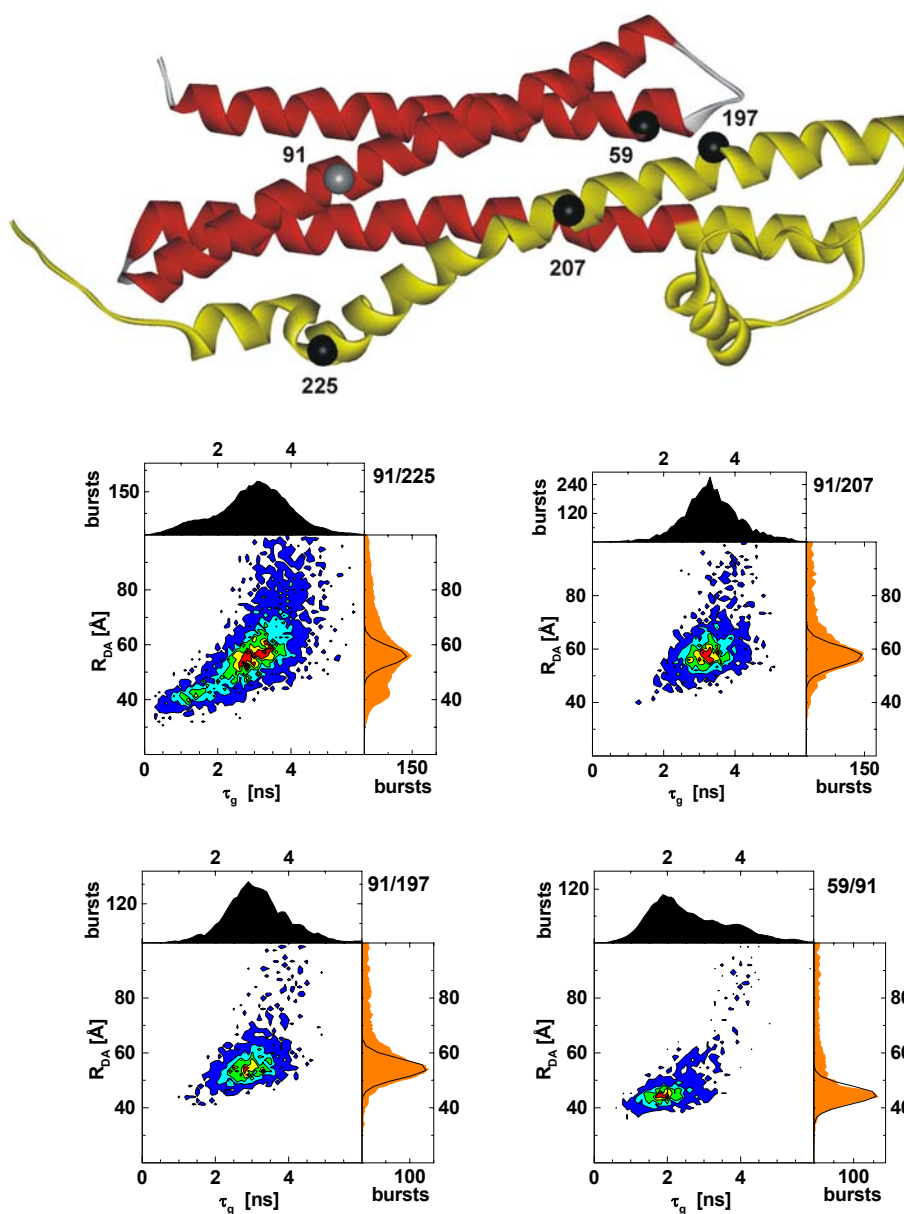


Fig. 16. Multi parameter fluorescence analysis of donor-/acceptor- labeled syntaxin mutants containing one cysteine in position 91 and a second one in a variable position

Upper panel: Crystal structure of syntaxin in complex with munc-18 (munc-18 not shown). The Habc-domain is depicted in red. The H3 domain and residues connecting it with the Habc domain are shown in yellow. The structure of this yellow marked part of the molecule is not known for isolated syntaxin. Spheres depict the α -carbons of cysteines. These are the amino acids which were labeled with Alexa488- and Alexa594-maleimide. All mutants contained a cysteine in position 91 (gray α -carbon). The second cysteine (black α -black) was located in one of the following positions: 59, 197, 207, or 225.

Lower panel: Two dimensional plots derived from the single molecule measurements of labeled double mutants Syx91/225, Syx91/207, Syx91/197, Syx59/91 (mutants are marked in upper right corner of plot). The central area depicts the accumulated bursts from donor-/acceptor- labeled proteins. Each burst is characterized by a specific lifetime τ_g and a distance R_{DA} that is derived from the intensity ratios of donor and acceptor fluorescence F_D/F_A . The frequency of bursts is color coded and increases from dark blue over light blue and yellow to red. The number of bursts is plotted either against lifetime (black, top) or distance (orange, right). For each major peak in the distance distribution a shot noise is determined (black curve, right) (see also “Methods”).

from the multi parameter analysis would give the best indication for dye/backbone interactions. The anisotropy values that were derived are all in the range between 0.15 and 0.25 (data not shown). Therefore, we conclude that the dyes are not firmly attached to the protein but rather represent rotational cones on the surface (preferred orientations of the rotational cones, though, cannot be excluded).

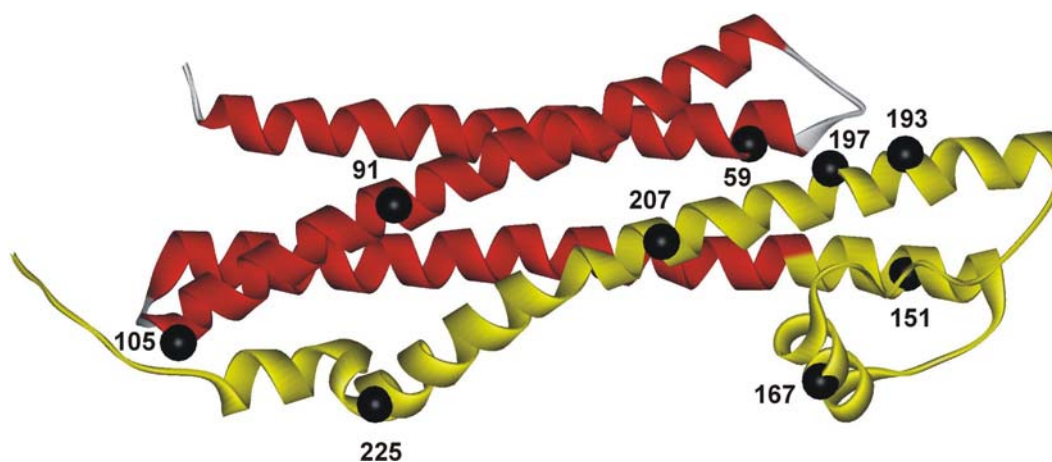
Burst analysis of each double mutant with respect to lifetime and intensity ratio of donor and acceptor dye is depicted in Fig. 16. Note that the distances given in the plot are computed from the fluorescence intensity ratios and were chosen as a scale to emphasize on the distance variability within each studied double mutant. The two dimensional plots encompass the accumulated information of all bursts in the respective measurement. For each mutant several thousands of fluorescence bursts were detected each of them representing a single molecule event. Interestingly, we observe no significant change in distance when comparing double mutants Syx91/225, Syx91/207 and Syx91/197 (see also Fig. 17). In all these mutants the second position is located in the H3 domain. In a closed syntaxin conformation one would expect an increase in distance.

Even for a fixed distance a distribution is expected that is due to intensity fluctuations. Such a curve is described by the shot noise (see methods) and depicted on the right of each plot. The burst distribution of Syx91/225 deviates significantly from this curve. Interestingly, we observe that the deviation decreases along the row Syx91/225, Syx91/207, Syx91/197, (see Fig. 17B for a comparison between shot noise and gauss fit). These results are evidence for an open conformation of syntaxin, with most conformational freedom at position 225 and successively decreasing freedom toward position 197. In the primary sequence amino acid 197 is closer to the Habc domain (residues 27-146) than amino acid 225. These 28 additional amino acids separating residue 225 from the Habc domain allow for greater motional freedom. Our control mutant in the Habc domain, Syx91/59, gave the sharpest peak of all. This result is in excellent agreement with the anticipated compact structure of the domain. Here, signal width appears to be influenced by dye mobility only.

In order to validate the data and to exclude effects of the label on the conformation of syntaxin additional positions were investigated. All distances with their respective shot noises and Gaussian fits (half widths) are summarized in Fig. 17.

The data support the above observations. First, double mutants within the Habc domain (Syx59/105 and Syx91/59) give sharp peaks due to narrow burst distributions, in

A



B

molecule (D/A)	syntaxin			syntaxin/munc-18
	R_{DA} [Å]	b [Å]	σ [Å]	crystal structure [Å]
Syx59/91	44.7	3.4	3.3	32.2
Syx59/105	57.6	3.8	3.2	51.6
Syx59/167	41.2	3.5	3.6	25.2
Syx59/197	49.0	6.3	3.4	14.2
Syx59/207	50.0	6.0	2.7	19.8
Syx59/225	41.8	3.0	2.8	
Syx59/225	53.3	6.9	3.2	38.5
Syx91/167	49.4	4.1	2.9	39.5
Syx91/193	52.5	4.2	4.1	42.4
Syx91/197	54.7	5.5	3.5	36.2
Syx91/207	58.0	6.5	3.8	22.4
Syx91/225	56.0	7.5	3.4	17.6
Syx105/197	41.0	3.7	3.4	
Syx105/197	9.6	5.2	3.8	55.7
Syx105/207	57.2	6.7	4.5	40.9
Syx105/225	56.0	10.0	4.5	17.7
Syx151/225	42.0	3.8	4.0	
Syx151/225	57.1	8.2	4.3	45.4
Syx167/197	46.2	4.4	3.2	17.8

Fig. 17. Distances between donor- and acceptor-fluorophores in syntaxin

(A) Structure of syntaxin in complex with munc-18 (munc-18 not shown). Positions that were labeled with Alexa488- and Alexa594-maleimide are depicted by black spheres (α -carbons).

(B) The table comprises all double mutants of syntaxin that were measured. The distances (R_{DA}) were derived from the intensity ratios of donor-/acceptor-fluorescence (F_D/F_A , see methods). For each mutant the half widths of the Gaussian fit (b) and the shot noise (σ) are included. For comparison, corresponding distances in the crystal structure (Misura *et al.*, 2000) are shown on the right. These distances are generally shorter because they are between α -carbons and not between fluorophores.

agreement with a stable three helix-bundle. Second, mutants that have labels on both the H3 and the Habc domains result in broad signals with half widths of the Gaussian fits generally decreasing in the row X/225, X/207, and X/197 (X = 59, 91, or 105). At the same time distance changes are rather small. Note that values given for syntaxin in complex with munc-18 represent distances between the C α -carbons. The dyes are connected to the protein backbone by a C5-linker, which has an extended length of 15 Å. Therefore, the absolute distances in the measured double mutants are expected to be larger. More important though are the relative distance changes between various double mutants in comparison to the known structure. To conclude, the distance information obtained from the accumulated FRET measurements agrees with a predominantly open conformation of syntaxin.

3.2.3.3 Multiple Conformations of Syntaxin

It is conceivable that the broad burst distributions observed for Syx91/225 and Syx105/225 reflect distinct conformations of the protein. The crystal structure of syntaxin in complex with munc-18 revealed that syntaxin is closed.

Our data of Syx91/225 in Fig. 16 contained a single shot noise curve. The two apparent maxima in the distribution though also allow the data to be represented by two curves. We now tested whether munc-18 binding to syntaxin results in a redistribution of the burst population, in short, a sharpening of the signal and disappearance of a peak. Complexes between labeled syntaxin and munc-18 or as a control labeled syntaxin, SNAP-25 and synaptobrevin were formed overnight on ice. In the case of the syntaxin/munc-18 complex the concentration of munc-18 was always kept at 2 micromolar to prevent dissociation of the protein at the picomolar concentrations used in the experiments. The ternary complex in contrast is stable enough not to dissociate. In each case complex formation was complete as monitored by SDS-PAGE and non-denaturing gel electrophoresis (Fig. 18A).

The two-dimensional histograms depicted in Fig 18B nicely demonstrate that in the ternary complex fluorescence resonance energy transfer is very poor. Here, position 225 is located in the middle of the complex on the surface of the four-helix bundle (EPR data). The Habc domain is structurally uncoupled. When the burst distribution of syntaxin bound to munc-18 is analyzed an overall shift with respect to lifetime and distance becomes apparent. In both cases the peaks with larger values disappear, strongly arguing for the existence of one

conformation. In the case of free syntaxin a broad distribution of bursts in both dimensions lifetime and intensity derived distance is observed. The donor/acceptor islands that are visible in the syntaxin/munc-18 complexes also appear in the corresponding free syntaxins but only as subpopulations. Bursts in these regions are very likely to represent syntaxin molecules in their closed conformation. A Gaussian fit through these bursts reveals that they comprise 15-30% of the total signal. Additional conformations could exist but are difficult to resolve. So far, both mutants of syntaxin that resulted in clearly distinguishable burst populations contained a fluorescent label in position 225. Interestingly, we found another double mutant that resulted in two peaks, namely Syx59/207. In the closed conformation this mutant resembles a pair on the opposite site of the four-helix bundle. Although peak separation is less obvious than in the examples above, munc-18 binding clearly effects the distribution of these conformational states. Complex formation results in a single sharp peak. In the ternary complex, too, only one peak is observed, but here it is very broad and shifted toward longer distances, in accordance with an open conformation and multiple structural states.

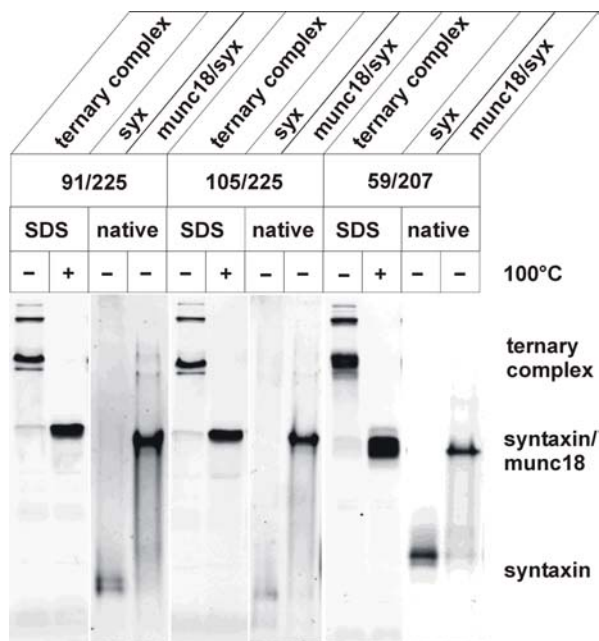


Fig. 18A. Donor-/acceptor-labeled syntaxins form stable complexes

(A) Complexes between syntaxin, synaptobrevin and SNAP-25 or syntaxin and munc-18 were analyzed by SDS-PAGE (15%) and native gel electrophoresis (8%), respectively. Syntaxins (labeled in positions 91/225, 105/225, or 59/207 with Alexa488- and Alexa594-maleimide) were detected by their fluorescence using an LAS detection system. Ternary complexes were either loaded directly or first heat-denatured. In all double mutants studied ternary complex formation and syntaxin/munc-18 complex formation was complete.

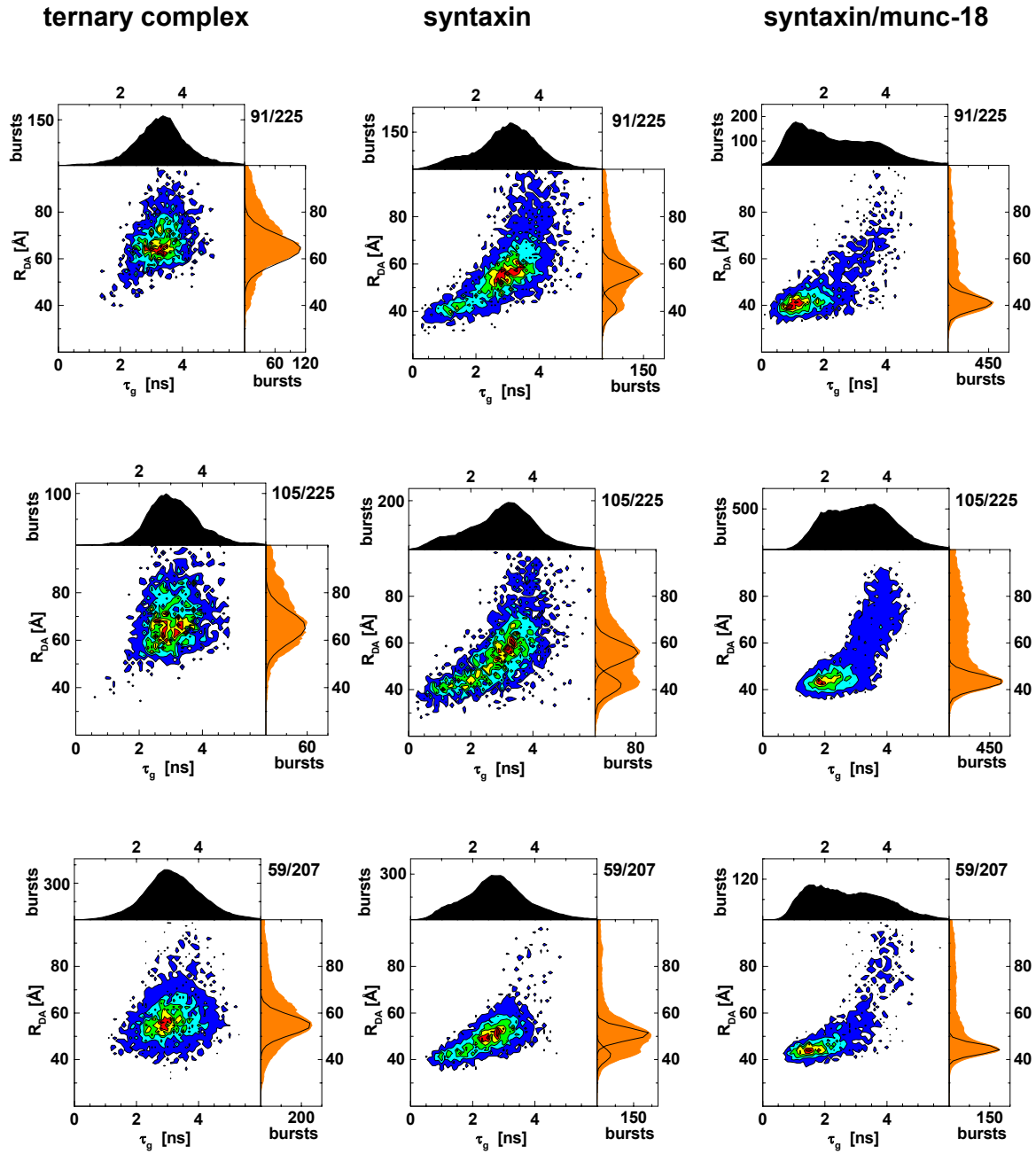


Fig. 18B. Multiple conformations of syntaxin

Two dimensional plots of double labeled Syx91/225, Syx105/225, and Syx59/207 either in complex with synaptobrevin and SNAP-25 (left), in isolation (middle) or in complex with munc-18 (right). The distance distribution (orange) reveals broad single peaks for ternary complexes, double peaks for isolated syntaxin and sharp single peaks for syntaxin/munc-18 complexes. In all cases shot noises are included. For color coding see Fig. 15.

Comparing the distances of isolated syntaxin in the row 105/225, 105/207 and 105/197 with those of complexes with munc-18 (table 4), reveals that in the latter case a successive increase occurs. In isolated syntaxin the distances are the same, supplying further evidence for a mainly open conformation of syntaxin.

	isolated syntaxin (measured)	syntaxin/munc-18 (measured)	syntaxin/munc-18 (crystal structure)
double mutant	[Å]	[Å]	[Å]
Syx105/225	56.0 42.0	43.5	17.7
Syx105/207	57.2	52.8	40.9
Syx105/197	59.6	64.9	55.7

Table 4. Distances between donor- and acceptor-fluorophores in free syntaxin and syntaxin in complex with munc-18. Values for free syntaxin are taken from Fig. 17B. For comparison distances between corresponding α -carbons in the crystal structure of the syntaxin/munc-18 complex are also shown.

3.2.3.4 A Kinetic Analysis of the Burst Distribution in Syx91/225

The analysis so far allowed distinguishing between open and closed states of syntaxin and their distribution. Next, the question arose whether an interconversion between the two conformations can be observed and on which time scale these structural changes may occur.

In order to resolve this question it was necessary not only to determine the mean parameters for each burst, but also to analyze the fluorescence parameters within the burst and if and how they change within the time of the burst duration.

Binning time analysis:

A binning time analysis was performed in which all bursts in the donor/acceptor island of Syx91/225 were analyzed according to different time intervals. To determine the fluorescence intensities only intervals that contained a minimum of 48 photons were selected. First, all donor/acceptor bursts were subdivided into 0.5 ms intervals. In Fig. 19 the number of time intervals is plotted against the distances. Two populations, characterized by two peaks in the red graph can be distinguished. When the interval size was increased to 1 ms, still, two populations were visible but the separation became less clear (green graph in Fig. 19). Increasing the time windows to 2, 3 and 4 ms resulted in the succeeding merger of both populations. These data clearly demonstrate that there is a

dynamic equilibrium between at least two different conformational states within the syntaxin molecules. At longer time intervals the two protein populations can not be separated any longer due to fluctuations and consequent averaging of the conformational information. The transition between the states takes place in a millisecond time range.

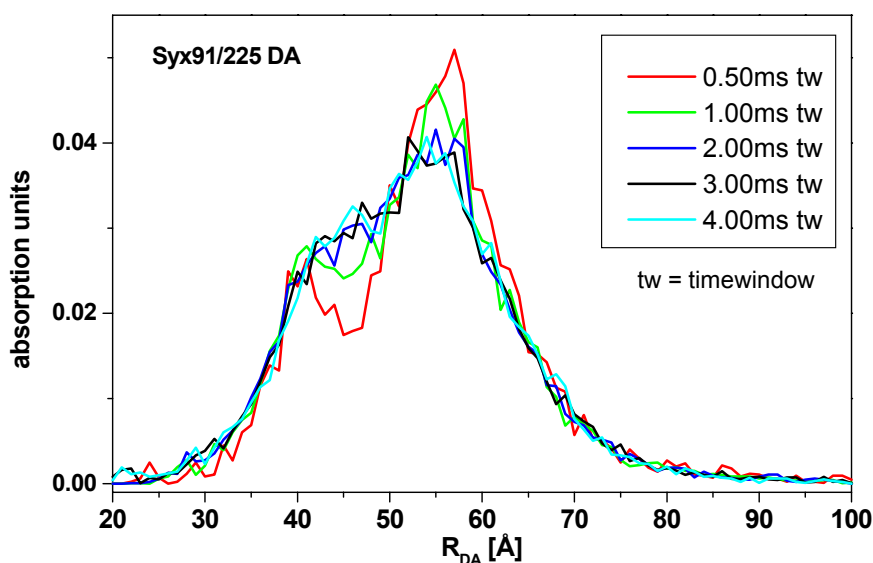


Fig. 19. Two populations of syntaxin seen by binning time analysis
The bursts for Syx91/225 (Fig. 16 and Fig. 17) are analyzed according to different binning times, with intervals ranging from 0.5 ms to 4 ms. Two visible populations at 0.5 ms merge into one with increasing time intervals, reflecting averaging of the distance information.

Fluorescence correlation analysis:

As a second approach, correlation analysis of the fluctuations of the donor and acceptor dye fluorescence within selected bursts was performed. The fluorescence bursts were selected based on the average value of F_D/F_A within the burst, so that only fluorescence from molecules labeled with both donor and acceptor dyes (DA- molecules) were used in the calculation of the autocorrelation function. In addition to fluorescence fluctuations due to translational diffusion of the molecules through the detection volume, and transitions to non-fluorescent transient photophysical states, fluctuations can also be expected in DA-molecules due to conformational changes within the molecules. For conformational changes in the presence of FRET, and if the distance between the donor and acceptor dyes decreases, a reduced donor fluorescence would be accompanied by an increased acceptor fluorescence intensity, and vice versa with increasing distances between

the dyes. An anti-correlation would occur between the donor and acceptor fluorescence intensities, where the relaxation time of the anticorrelation reflects the time scale of the intramolecular motion, and its amplitude scales with the difference in donor-acceptor distances between the intramolecular states. Correlation analysis of selected bursts makes it possible to characterize conformational changes, or other dynamic processes, taking place within a broad dynamic time range. In Fig. 20, three correlation curves for the DA-molecules of Syx91/225 are shown, the green-to-green (Ggg), and the red-to-red (Grr) fluorescence autocorrelation, as well as the green-to-red fluorescence crosscorrelation (Ggr) curves. For Ggr a significantly longer overall decay time of the correlation curve could be observed compared to those of Grr and Ggg. This can be attributed to the contribution of an anti-correlation between the green and the red fluorescence having a time scale of approximately 0.7 ms. A corresponding anticorrelation was also found for Syx105/225 (data not shown), not though for mutants showing a confined distribution of parameter values in the 2D cumulative histograms. The selective correlation analysis

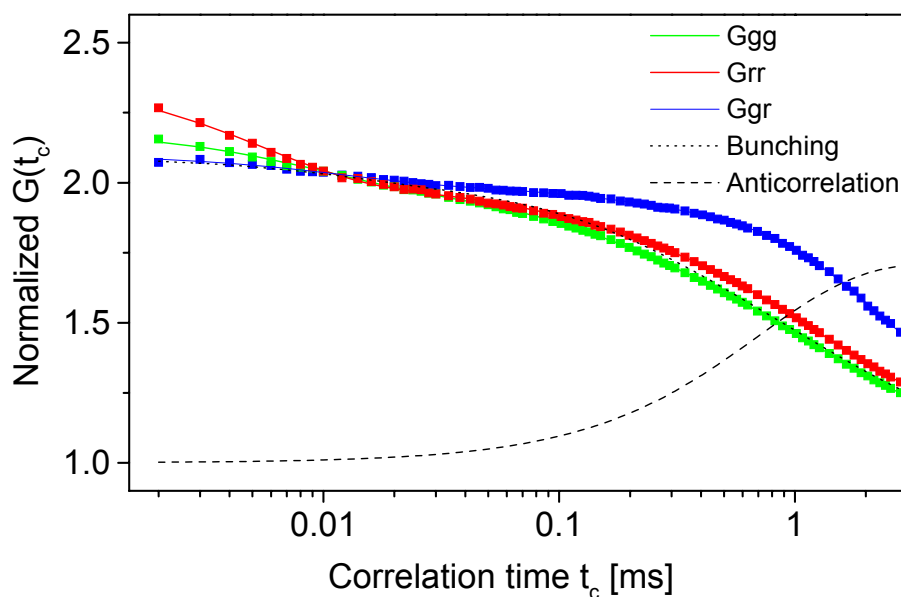


Fig. 20. Structural fluctuations in syntaxin observed by Fluorescence correlation spectroscopy Plot of normalized diffusion against correlation time. Autocorrelation of the red and green components in the donor-/acceptor-island of Syx91/225 yield similar results (Grr and Ggg). Dotted line is a mean autocorrelation curve that is corrected for bunching. Cross correlating red and green fluorescence (Ggr) yields and increase in the apparent diffusion time. The anticorrelation (dashed line) indicates that open and closed states of Syx91/225 fluctuate within 0.7 ms. For time ranges down to $\sim 10\mu\text{s}$ no anticorrelation is observed.

provides supporting evidence to the binning time analysis above that the syntaxin molecules are in a dynamic equilibrium, with conversion in the millisecond time range. Furthermore, for time ranges down to $\sim 10 \mu\text{s}$, no additional anticorrelation could be observed, indicating that no significant conformational changes take place within this faster time range.

3.3 Interactions between Syntaxin and Synaptobrevin Involving the Transmembrane Domains

3.3.1 General Remarks

Most of the structural studies on SNARE proteins were carried out using soluble versions of the proteins. It is often thought that single membrane spanning α -helices merely serve as featureless hydrophobic anchors. That this is generally not the case has been demonstrated for a great number of proteins ((Lemmon & Engelman, 1994) for review)). Helix-helix interactions may serve to stabilize membrane protein complexes. In the influenza fusion protein hemagglutinin it was shown that the membrane anchor is required for membrane fusion. When the transmembrane region was substituted for a GPI anchor, which perfectly retained the protein in the membrane hemifusion but not complete fusion was observed (Kemble, Danieli & White, 1994).

It is conceivable that the membrane regions of syntaxin and synaptobrevin also interact. In fact, for synaptobrevin it was shown that the protein could form specific dimers (Laage & Langosch, 1997).

Here, the question is raised whether syntaxin, too, is capable of forming stable dimers. Furthermore, it is asked whether an interaction between syntaxin and synaptobrevin exists that is mediated by the transmembrane domains.

The above single molecule measurements revealed, that syntaxin folds back only partially. Additionally, the EPR studies showed that the SNARE motif of syntaxin could form homooligomers. An equilibrium between homooligomerized syntaxin in an open conformation and monomeric syntaxin in a closed conformation is conceivable. Interactions between transmembrane regions may be important to shift these equilibria.

In order to study the interactions between syntaxin and synaptobrevin molecules in membranes recombinant versions of both full-length proteins were reconstituted into artificial lipid bilayers (for a methodological review on protein reconstitution see (Rigaud, Pitard & Levy, 1995)).

3.3.2 Interactions between the Transmembrane Domains of Syntaxin and Synaptobrevin

Recombinant full-length syntaxin 1a and synaptobrevin 2 containing a C-terminally added His₆-tag were expressed in *E. coli* and purified by Ni-NTA affinity chromatography in the presence of 1.5% (w/v) cholate as detergent. After addition of cholate-solubilized phospholipids, the proteins were co-reconstituted in liposomes by detergent removal using size exclusion chromatography. The proteoliposomes eluted at the void volume and were dialyzed overnight to remove any residual detergent. When the proteins in the proteoliposome fraction were analyzed by SDS-PAGE and immunoblotting, several protein bands with an apparent Mr higher than that of the monomers were detected (Fig. 21).

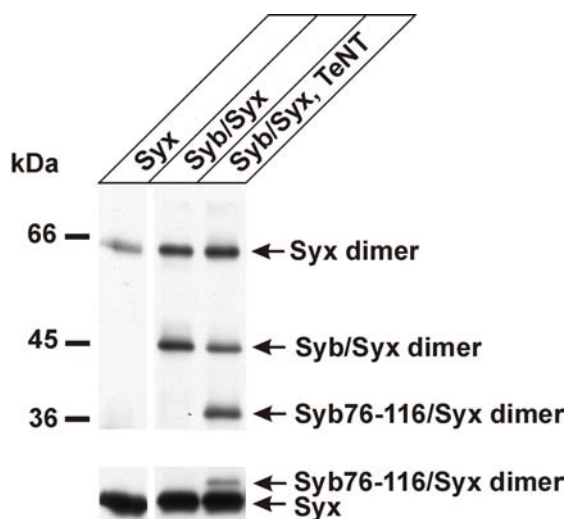


Fig. 21. Co-reconstitution of synaptobrevin 2 and syntaxin 1a into proteoliposomes leads to the formation of a SDS-resistant heterodimer (Syx/Syb dimer) that is partially cleaved by TeNT light chain. All samples were analyzed by SDS-PAGE and immunoblotting, using a mixture of monoclonal antibodies 69.1 (synaptobrevin 2) and HPC-1 (syntaxin 1) for detection. Left lane, proteoliposomes reconstituted with syntaxin 1a; middle lane, co-reconstitution of synaptobrevin 2 and syntaxin 1a; right lane, co-reconstitution of synaptobrevin 2 and syntaxin 1a, followed by digestion with TeNT light chain. Top panel: 8% separation gel; lower panel: 14% separation gel (to show equal loading of syntaxin). Note that a syntaxin homodimer (Syx dimer) is also observable.

In addition to a syntaxin dimer, a complex between syntaxin and synaptobrevin was observable that migrated at an apparent Mr of 45,000 (Fig. 21). This complex was also detectable when the blot was incubated separately with either anti-syntaxin or anti-synaptobrevin antibodies (not shown). Digestion of the proteoliposomes with tetanus toxin (TeNT) light chain, which resulted in a partial cleavage of synaptobrevin (not shown, (Link *et al.*, 1992), led to the appearance of an additional band of lower Mr (Fig. 21) that

probably consists of an adduct between syntaxin and the C-terminal membrane anchored fragment of synaptobrevin.

These data indicate that synaptobrevin and syntaxin form a 1:1 complex in proteoliposomes that is at least partially resistant to SDS and that involves the C-terminal end of synaptobrevin. To investigate whether the transmembrane domain of syntaxin is participating in this interaction, we expressed a truncated, epitope (myc)-tagged version of syntaxin that corresponds to the C-terminal cleavage product of botulinum neurotoxin C1 (Schiavo *et al.*, 1995) and that contains only 12 amino acid residues in addition to the transmembrane domain. As shown in Fig. 22, co-reconstitution of this fragment with full-length synaptobrevin resulted in the formation of a complex that was detectable with both anti-synaptobrevin and anti-myc antibodies. The complex migrated with an apparent Mr of 23,000, i.e. a Mr expected for a 1:1 complex between synaptobrevin and the syntaxin fragment. Together, these data demonstrate that syntaxin and synaptobrevin form a stable binary complex upon co-reconstitution in liposomes. Complex formation was dependent on the two proteins being present in the same membrane. When synaptobrevin and syntaxin 1a were reconstituted into separate liposome populations and mixed subsequently, no complex formation was observed (not shown). This also demonstrated that the complex did not form after addition of SDS.

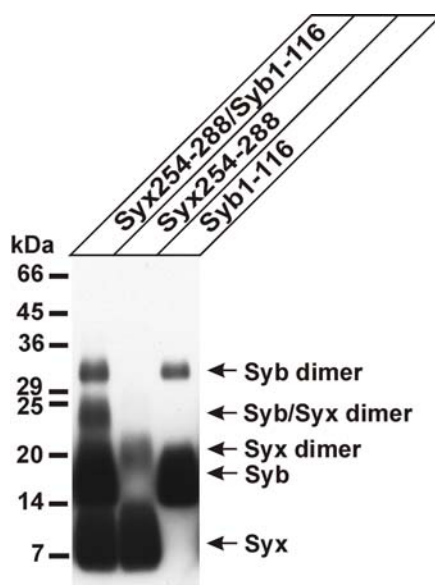


Fig. 22. Heterodimer formation after reconstitution of synaptobrevin with an N-terminally truncated version of syntaxin 1a (left lane). Analysis was performed as in Fig. 21 except that an anti-myc antibody was used instead of HPC-1. Both, truncated syntaxin 1a and synaptobrevin form homodimers (middle and right lane) that are separated from the heterodimer.

concentration was increased well above the critical micelle concentration, the amount of complex was reduced. This was expected because the proteins are dissolved in detergent micelles instead of being concentrated in the membrane. Similar results were obtained when synaptobrevin-containing proteoliposomes were digested with TeNT light chain, followed by centrifugation and resuspension, before syntaxin was added. Again, a complex was observed at 0.6% (w/v) octylglucoside, which was reduced upon solubilizing the liposomes (Fig. 23, lower panel).

In the next series of experiments, we investigated whether the binary syntaxin-synaptobrevin interaction is detectable after NSF-driven disassembly. A preformed ternary complex, consisting of full-length syntaxin, synaptobrevin, and SNAP-25, was reconstituted into proteoliposomes. In the first experiment, the liposomes were incubated in the presence of NSF and α -SNAP under conditions that either block or favor disassembly. Analysis of the protein complexes by SDS-PAGE revealed that partial disassembly of the ternary complex (visible as a major band migrating at a Mr of 60,000) induced the formation of the synaptobrevin-syntaxin complex (Fig. 24, left).

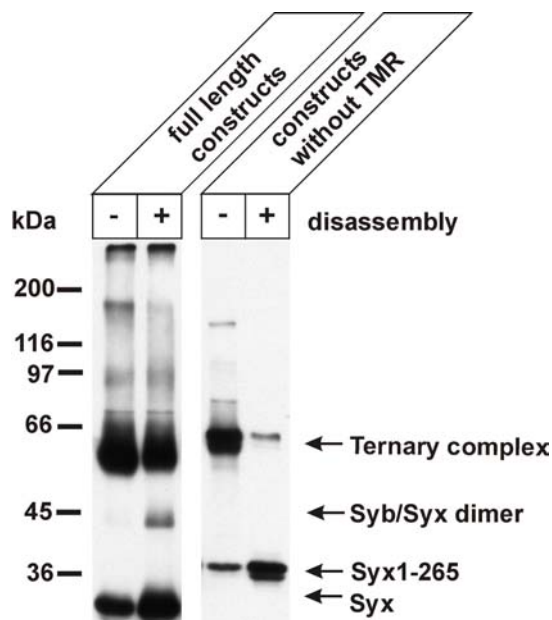


Fig. 24. Disassembly of the ternary SNARE complex in proteoliposomes by α -SNAP and NSF leads to the formation of a syntaxin/synaptobrevin heterodimer. Synaptobrevin and syntaxin were expressed either as full-length proteins (left lanes) or as truncated proteins lacking their transmembrane domains (right lanes) and combined with recombinant SNAP-25 to form ternary SNARE complexes. The complex containing full-length proteins was reconstituted into proteoliposomes. Note that no dimer is formed upon disassembly of the truncated complex. Syntaxin without transmembrane domain migrates slower than its full-length counterpart. This is due to the presence of a larger tag.

As control, an identical experiment was carried out with ternary complex formed from recombinant proteins lacking their transmembrane domains. As expected, no syntaxin-synaptobrevin complex was observed (Fig. 24, right).

3.4 Formation of trans-SNARE Complexes

A central part of the zippering model of SNARE mediated membrane fusion is that SNARE proteins on apposing membranes come together to form trans SNARE complexes. Once the membranes are fused the SNARE complexes are considered to be cis. Here, we asked whether it is possible to obtain biochemical evidence for the existence of these trans complexes.

SNARE complex formation can be inhibited by the monoclonal antibodies 71.1 and 71.2, which bind to amino acids 20-40 and 1-20, respectively (Bruns *et al.*, 1997). Inhibition of complex formation is more efficient by Cl. 71.1. The antibody binds to a region in SNAP-25 that is part of the SNARE motif.

The inhibition of complex formation can be observed in our fluorescent anisotropy assay. When 4 nM of Alexa488 labeled SNAP-25 (position 84) was preincubated for 3.3 min with 500 nM of a Fab fragment of 71.1, complex formation was significantly hindered. The addition of an almost thousand fold excess of syntaxin and synaptobrevin resulted in a very slow rise in anisotropy when compared to the control reaction (Fig. 25).

71.2 also interfered with complex formation although to a markedly lesser degree (not shown). Extending the preincubation time to 10 min did not change the kinetics (data not shown). Therefore, we conclude that antibody binding was complete.

Next we investigated whether complex formation is inhibited when the proteins are inserted into lipid bilayers. It has been reported that mixtures of proteoliposomes containing syntaxin 1a/SNAP-25 and synaptobrevin, respectively, display SNARE-dependent interactions, including membrane fusion (Weber *et al.*, 1998). Thus this experimental approach should provide an *in vitro* assay for complexes that, at least initially can only interact in the trans configuration. Full-length versions of both syntaxin 1A and synaptobrevin 2 were reconstituted by detergent removal into separate sets of liposomes. Analysis of the proteoliposomes by floatation gradients revealed that the proteins were quantitatively incorporated into vesicles, with no free protein left behind in solution. Furthermore, both proteins were almost exclusively oriented with their cytoplasmic

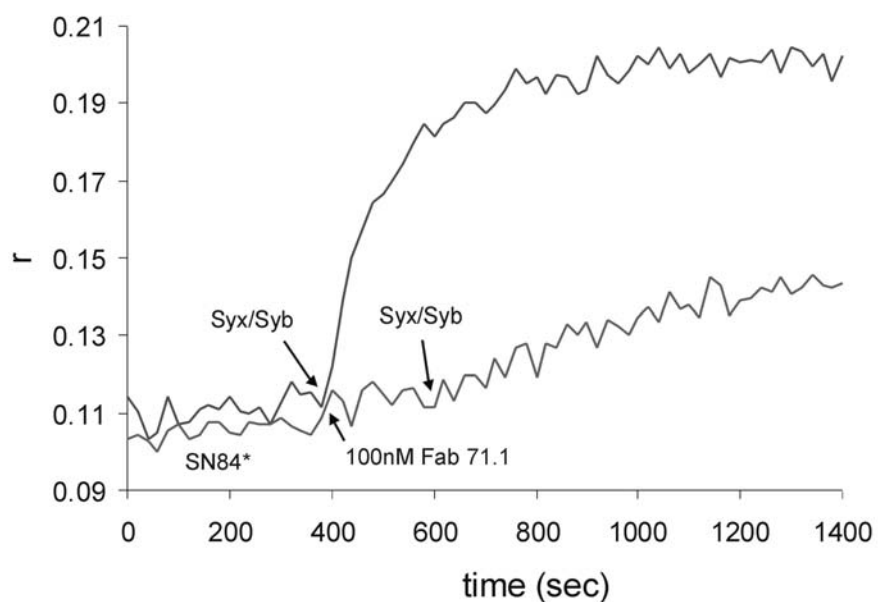


Fig. 25. Inhibition of ternary complex formation by Fab 71.1 (anti SNAP-25)
 Addition of a synaptobrevin (3.2 μ M)/syntaxin (16 μ M) mixture to SNAP-25 (5 nM, labeled at position 84 with A488-maleimide) results in ternary complex formation. The process can be monitored by a change in fluorescence anisotropy (r) (see also Fig. 14B). When SNAP-25 is incubated for 3.3 min with 100 nM Fab 71.1 prior to complex formation a significant slow down of the reaction is observed.

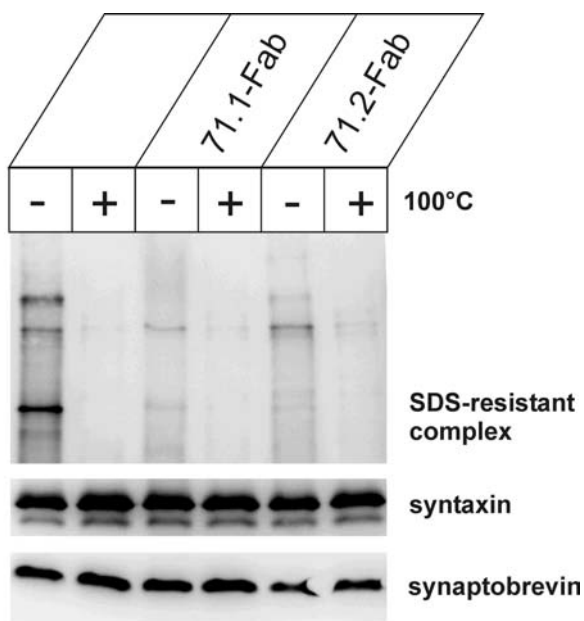


Fig. 26. Fab fragments of Cl. 71.1 and Cl. 71.2 prevent SNARE interactions in membranes.
 Proteoliposomes containing either syntaxin 1A or synaptobrevin 2 were mixed with SNAP-25A that was preincubated with buffer or the respective Fab fragments. Complex formation is monitored by the appearance of SDS resistant bands (top panel: 8% gel, bottom panel: 15% gel). Note that the apparent molecular weight of the major complex is higher than that of the soluble complex and correspond to that of complexes isolated from native membranes (see e.g., Otto *et al.*, 1997).

domains facing the outside of the vesicles (tested by limited proteolysis, data not shown). These liposomes were then mixed and recombinant SNAP-25 was added. Incubation resulted in the formation of SDS resistant complexes (Fig. 26).

No complexes were seen when SNAP-25 or one of the liposome populations were omitted (data not shown). Again, complex formation was prevented by preincubation of SNAP-25 with Fab fragments derived from the SNAP-25-specific monoclonal antibodies (Fig. 26). Since all incubation steps were performed on ice and membrane fusion is effectively stopped by low temperature we conclude that the SNARE complexes formed represent trans-complexes.